

Zero-Parameter Model of the N - N Potential*

HIROTAKA SUGAWARA

Department of Physics, University of California, Berkeley, California 94720

AND

FRANK VON HIPPEL

Institute of Theoretical Physics, Department of Physics, Stanford University, Palo Alto, California 94305

(Received 9 October 1967)

We present a theoretical N - N potential containing, in addition to the one-pion-exchange contribution, vector-meson-exchange terms and contributions due to the inelastic interactions $N+N \rightarrow N+\Delta(1236)$ and $N+N \rightarrow \Delta(1236)+\Delta(1236)$. There are no adjustable parameters in this calculation, which otherwise, however, suffers from most of the usual shortcomings and difficulties of few-particle-exchange models for strong-interaction processes. The vector-meson coupling constants are fixed by electromagnetic form factors and backward vector-meson production data, while the phenomenological constants in the inelastic contributions to the potentials have been fixed by the experimental data on the inelastic reactions themselves. Our results are found to be in qualitative agreement with phenomenological potentials obtained by Reid from the N - N scattering data. We also calculate the vector-meson-exchange potentials for all B - B and B - \bar{B} states with $J \leq 2$. Our results indicate that the B - B interaction will contain a short-range repulsion in all states of practical interest aside from the $T=1$ Ξ - N state which is discussed. We find strong attractions in most of the $SU(3)$ singlet and octet B - \bar{B} states.

1. INTRODUCTION

IN this paper a crude but zero-parameter calculation of some contributions to the nucleon-nucleon interaction is presented. We find that these contributions can account for many of the qualitative features of the experimental N - N scattering data, although our *quantitative* fit to the data would be very poor when compared to that of models containing up to a dozen adjustable parameters (coupling constants, meson masses, cutoffs, etc.).

Our model is based largely on ideas which have evolved over the past 30 years as a residue of the many theoretical attempts to understand the N - N interaction. In some respects it does not come up to the standards of sophistication which have been achieved by other model calculations of the N - N interaction. Therefore we do not see our calculation as supplanting these previous calculations, but rather we hope that it will complement them.

In particular, we have not expressed our ideas in the language of dispersion theory, into which it appears that any correct calculation must ultimately be cast. Instead we have chosen to express our results in terms of energy-dependent potentials. We make this choice because we have no solutions for the technical difficulties encountered in the dispersion-theoretic calculations.

We believe that our contribution lies in two other areas:

(i) It appears to us that it is now possible, as the result of much experimental and theoretical work, to make reasonable estimates of the vector-meson couplings of the nucleons without using the N - N scattering data. We have made these estimates and show in this

paper that the predictions for the form of the short-range N - N interaction obtained by using these coupling constants are not in gross disagreement with experiment.

(ii) We have made an approximate calculation of the effects on elastic N - N scattering of the inelastic reactions $N+N \rightarrow N+\Delta(1236)$ and $N+N \rightarrow \Delta(1236)+\Delta(1236)$. These effects have been considered before but always by approximating the inelastic amplitudes as due to one-pion exchange. This gave rise to effective potentials which were very singular for small separations, leading one to wonder whether it made sense to ascribe the short-range N - N interaction to vector-meson exchange. We find that when one modifies the one-pion-exchange (OPE) $N+N \rightarrow N+\Delta$ and $N+N \rightarrow \Delta+\Delta$ amplitudes so as to obtain better fits to production experiments, their contribution through unitarity to the N - N potential is much less singular and requires no further cutoff. It appears from our results that that N - N attraction due to the effect of these higher inelastic channels may account for a substantial amount of the attraction usually parametrized by a scalar-meson exchange.

In order to see how well the contributions which we have calculated reproduce the "long-range," "intermediate-range," and "short-range" N - N interactions, we have derived from them an energy-dependent potential for the N - N interaction in each eigenstate of spin-parity and total angular momentum. We compare these potentials to the phenomenological potentials which Reid¹ constructed to give the N - N elastic-scattering phase shifts for $J \leq 2$.

¹ R. Reid, thesis, Cornell University (unpublished).

² We do not calculate the η -exchange contribution. For an $SU(3)$ D/F coupling ratio near $3/2$, it will be unimportant at short range in comparison to the vector-meson-exchange potentials because of the small η coupling constant [$(g_{\bar{p}p\eta})^2 \approx 0.1(g_{\bar{p}p\pi})^2$]. It is unimportant for larger N - N separations because of the large η mass.

* Research sponsored by the Air Force Office of Scientific Research, Office of Aerospace Research, U.S. Air Force, under AFOSR Contract No. AF 49(638)1389 and AFOSR Grant No. AF-AFOSR-232-66.

Our effective potential is the sum of three parts: (1) the one-pion exchange potential (OPEP),² (2) an energy-dependent vector-meson-exchange potential which, in Born approximation, gives back the one-vector-meson-exchange Born amplitude (the vector-meson-nucleon coupling constants are estimated from electromagnetic-form-factor and vector-meson-production data in Sec. 2), and (3) an energy-dependent "coupled-channel" potential, which represents the effective attractive potential below the inelastic threshold due to the reactions³

$$(II) \quad N+N \rightarrow N+\Delta(1236),$$

$$(III) \quad N+N \rightarrow \Delta(1236)+\Delta(1236).$$

Reaction II dominates the inelastic N - N interactions up to quite high energies⁴ and would therefore play an important role in any dispersion treatment of N - N scattering. The reaction appears to proceed dominantly via OPE,⁵ and it has been suggested that reaction III does also.⁶ The contributions of these reactions, through inelastic unitarity on the N - N scattering amplitude, will therefore have important singularities in the momentum-transfer variable corresponding to two-pion exchange. Thus our coupled-channel potential may be thought of as constituting an estimate of the uncorrelated two-pion-exchange contribution to the N - N potential. We do not expect the production of the higher-spin nucleon resonances to make individual contributions to low-energy N - N scattering comparable to those due to reactions II and III. (However, the new s - and p -wave π - N resonances may make a substantial contribution.⁷)

³We have labeled these reactions II and III, respectively, to distinguish them from the elastic scattering reaction I: $N+N \rightarrow N+N$.

⁴See D. V. Bugg, D. C. Salter, G. H. Stafford, R. F. George, K. F. Riley, and R. L. Tapper, Phys. Rev. **146**, 980 (1966), where earlier references may be found.

⁵See, e.g., E. Ferrari and F. Selleri, Nuovo Cimento **27**, 1450 (1963).

⁶See, e.g., E. Ferrari, Nuovo Cimento **30**, 240 (1963).

⁷The longest-range contributions of these inelastic processes to the N - N interaction are due to production via OPE. A relevant measure of the strength of the coupling of the higher resonances to the π - N channel is the quantity $\Gamma_{R^*} \equiv \Gamma_{\pi N^*} (M_{\pi}/q)^{2l+1}$, where $\Gamma_{\pi N^*}$ is the partial width of the resonance into the π - N channel, l is the orbital angular momentum in the final state, q is the momentum of the decay pion in the c.m. system, and M_{π} is of the order of the momentum transfers contributing to the N - N intermediate-range attraction. The value of Γ_{R^*} is orders of magnitude smaller for resonances with $l > 2$ than it is for the s - and p -wave resonances. Among these latter resonances Γ_{R^*} is about a factor of 2 larger for the $\Delta(1236)$ than it is for the higher resonances. This, along with the fact that the $\Delta(1236)$ is the least massive of the resonances, guarantees the relative importance of reactions II and III to elastic N - N scattering. For the more massive resonances, the contribution of double-resonance production to the intermediate-range attraction should be more important than that of single-resonance production. Single-resonance production requires an energy transfer $\Delta E = (M^{*2} - M^2)/4E$ between the baryons in the c.m. frame, where M and M^* are, respectively, the masses of the nucleon and resonance and E is the initial c.m. energy of the nucleon (of the order of M^*). It will be seen in Appendix B that the range of the corresponding N - N interaction goes as $\frac{1}{2}[(\Delta E)^2 + (M_{\pi}^2)]^{-1/2}$. Thus it becomes smaller as M^* increases.

It is obvious that there are any number of effects contributing to the N - N potential which we have not considered. Examples include (a) the enhancement of the amplitude for exchanging a low-mass π - π pair because of a possible strong attractive s -wave π - π interactions, (b) crossed two-pion-exchange diagrams, (c) the exchange of mesons with masses greater than 1 BeV/ c^2 , and (d) the effect of the inelastic production processes leading to final states other than those of reactions II and III. At our present stage of sophistication and experimental knowledge we cannot make a realistic zero-parameter calculation of these contributions. There is room for contributions such as (a) and (d) in our theoretical potentials, in that most of them are somewhat less attractive than Reid's at intermediate ranges or are so strongly repulsive in this range that they would not be much affected by the addition of a reasonable amount of attraction from these sources.

In the following subsections we discuss our major results. The derivations of the vector-meson-exchange and coupled-channel potentials are discussed in Sec. 2 and Appendix A and in Sec. 3 and Appendix B, respectively.

Nucleon-Nucleon Potential Results

In Fig. 1 we display Reid's phenomenological energy-independent potentials and our theoretical energy-dependent potentials. The two theoretical potentials shown correspond to the extremes of the N - N elastic scattering energy interval: N - N threshold and N - N - π threshold, respectively. OPE potential has been taken out of all the potentials shown in Fig. 1. Thus, only the unknown parts of the phenomenological potential are being compared to our vector-meson-exchange plus coupled-channel potential. In general the short-range parts of the potentials ($r < 0.5\mu_{\pi}^{-1}$) are dominated by the vector-meson-exchange contributions. In the intermediate range, $0.5\mu_{\pi}^{-1} \leq r \leq \mu_{\pi}^{-1}$, the vector-meson-exchange and the coupled-channel potentials are of the same order of magnitude. In the $r > \mu_{\pi}^{-1}$, the coupled-channel contribution dominates, because the OPEP has been taken out.

It will be seen that on all the plots corresponding to scattering states with nonzero orbital angular momentum, the abscissa has been divided into two intervals by a vertical shaded line. This shaded line defines a "comparison radius," outside of which we believe a quantitative comparison of the theoretical and phenomenological potentials is meaningful. The comparison radius has been placed, to the nearest tenth of a pion Compton wavelength, at the point where Reid's potential, including the OPEP plus the centrifugal barrier, exceeds 200 MeV repulsion. Reid found that the calculated phase shifts are insensitive to wide variations of the form of the phenomenological potentials inside this radius.

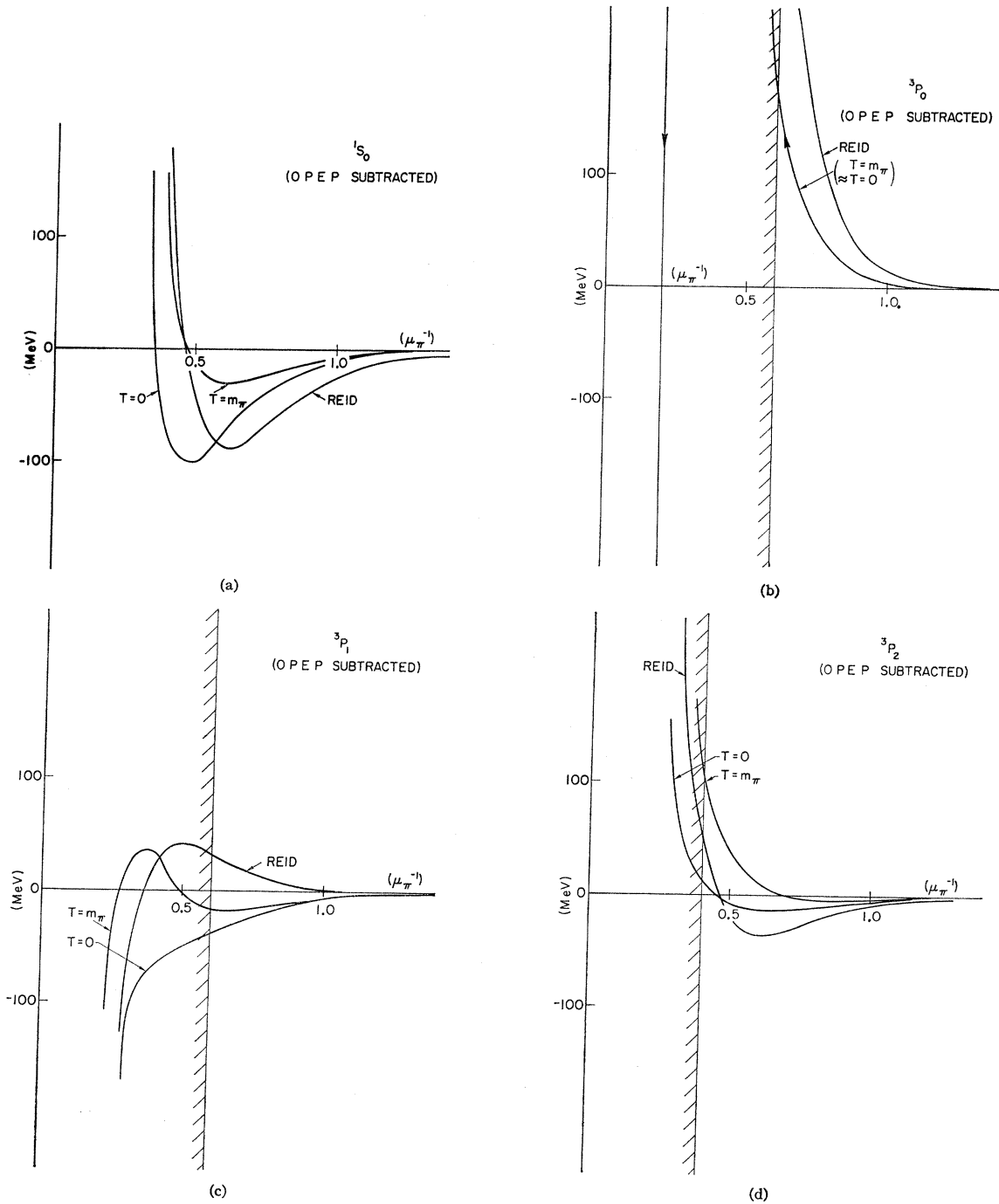


FIG. 1. Theoretical and phenomenological potentials for all $N-N$ states with $J < 2$. The line labeled "Reid" in each figure is a phenomenological potential which gives the experimental phase shifts. The other curve or curves are our calculated potentials. When the theoretical potential has a strong energy dependence, it is drawn for the two extremes of the elastic scattering energy interval: $N-N$ threshold ($T=0$) and pion-production threshold ($T=m_\pi$). The vertical shaded barrier in some of the figures shows the "comparison radius," inside which Reid's potentials are insensitive to the experimental phase shifts.

We should state here that, because of the nonunique relationship between the vector-meson-exchange Born amplitude and the vector-meson-exchange potential, there is some uncertainty in these potentials. As will be discussed in Sec. 2, the uncertain terms are important

only in the 1S_0 and 3S_1 potentials and not in the potentials corresponding to states with nonzero orbital angular momentum. Our derivation has led to the potentials shown. The reader is referred to Sec. 2 and Appendix A for a further discussion of this point.

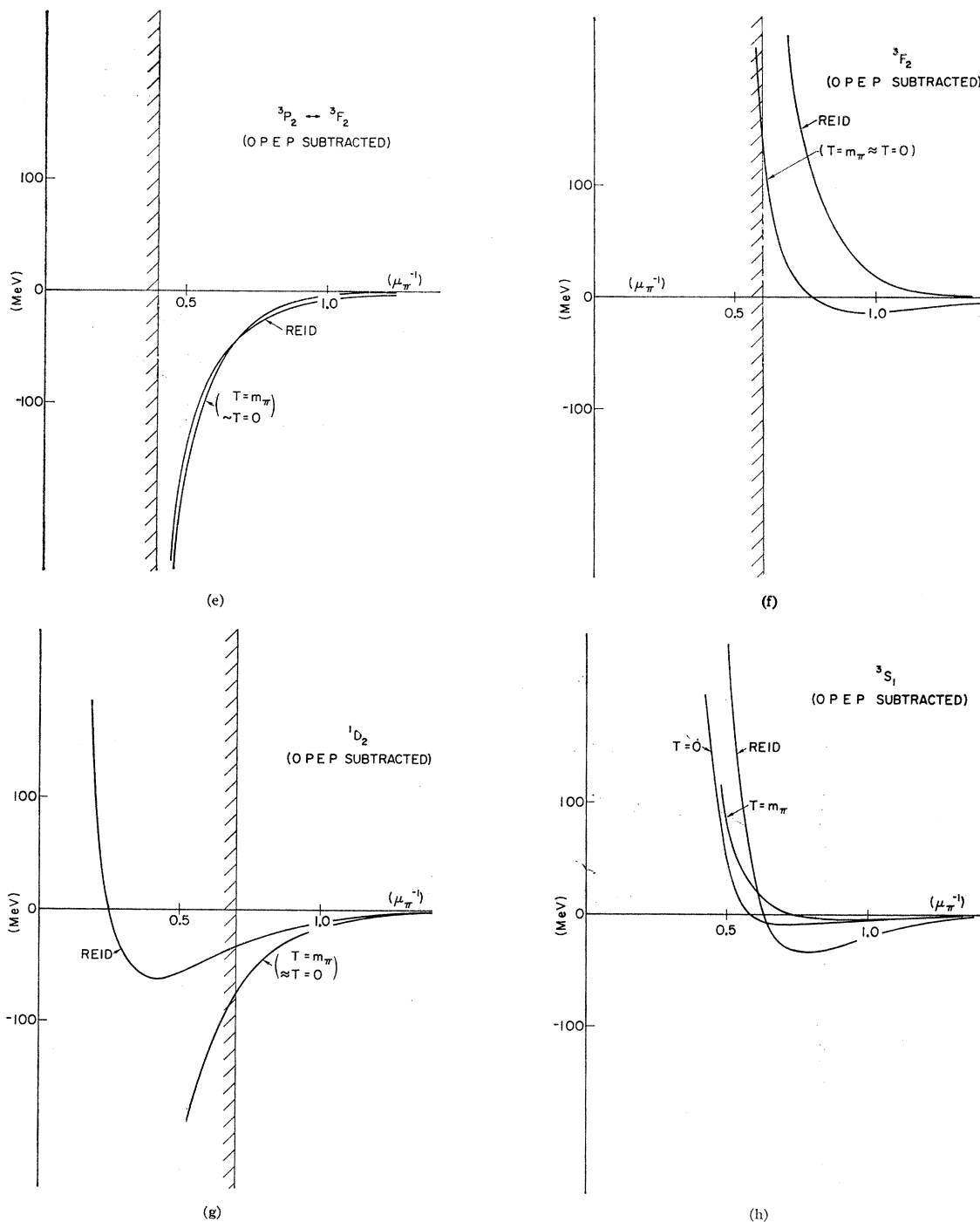


FIG. 1 (continued)

It can be seen from the figures that, outside the comparison radius, there is substantial qualitative agreement between Reid's potentials and our own. We discuss here each of the potentials in turn and interject some general comments.

1S_0 : In the 1S_0 state we have the short-range repulsion and intermediate-range attraction characteristic of all

phenomenological static potentials which have been used to fit the 1S_0 phase shift. The short-range repulsion has almost the same range as that in Reid's 1S_0 potential. Our intermediate-range attraction has a very strong energy dependence. This is because of a strong cancellation between the repulsive vector-meson-exchange and attractive coupled-channel potentials in

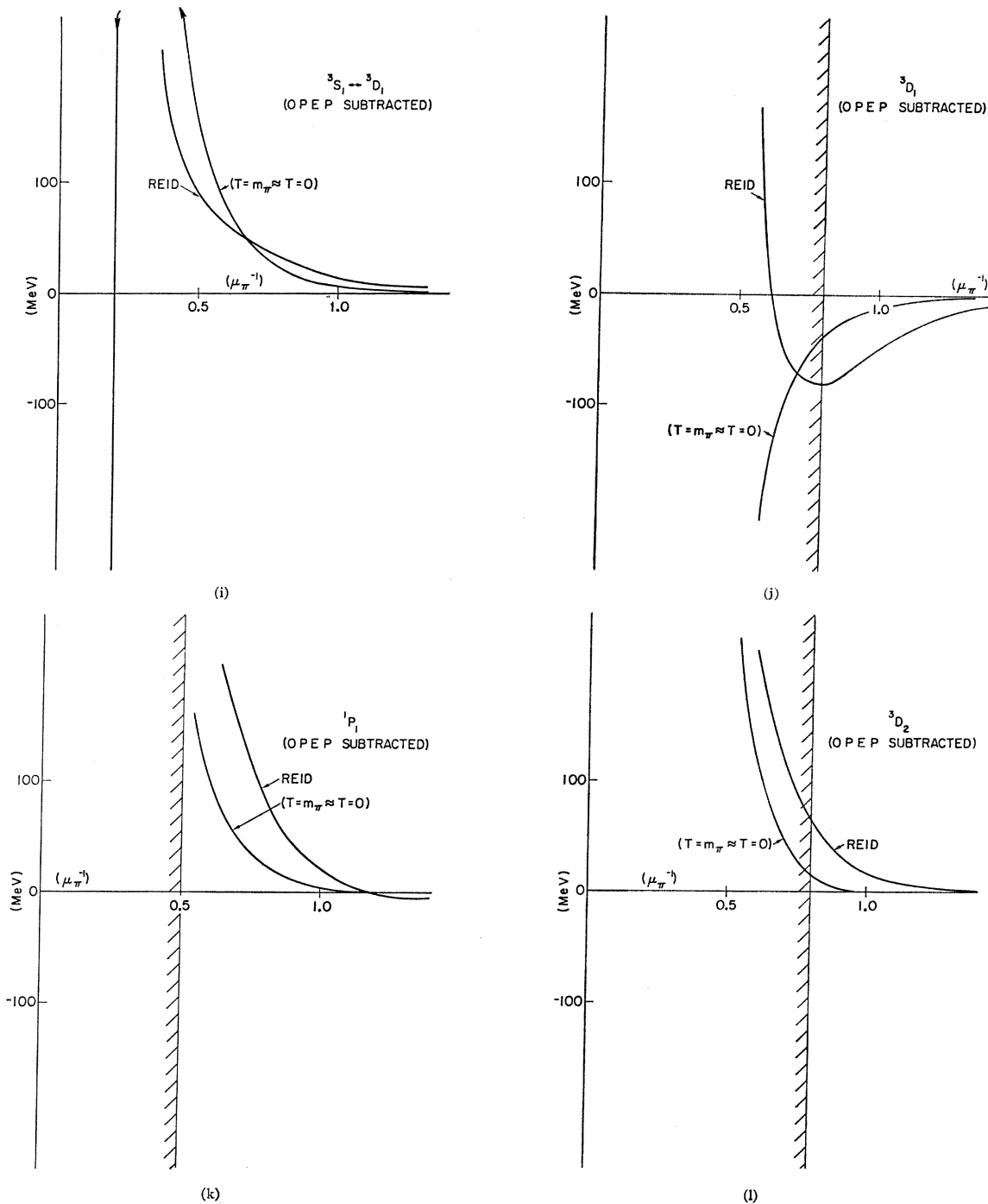


FIG. 1 (continued)

this range; although each of these potentials has an energy dependence of only about 30% between N - N and N - N - π thresholds, their sum varies by much more. At long range our potential is smaller than Reid's. This will be seen below to be a characteristic of a large number of our partial-wave potentials. It is not clear at this stage whether this merely is a characteristic of Reid's parametrization of the partial-wave potentials

or whether, indeed, the more slowly decreasing, stronger long-range behavior is required.

3P_0 : It can be seen that here there is good qualitative agreement between Reid's potentials and our own. The strength of the vector-meson repulsion is overwhelming and there is, therefore, relatively little energy dependence.

3P_1 : This is a peculiar case. It may be seen that the

phenomenological potential is attractive at long range, repulsive at intermediate range, and attractive again at short range. We believe that the short-range attraction may be due to the nature of Reid's parametrization. The OPE tensor potentials produce a very strong repulsion in the 3P_1 state, going as r^{-3} for small r . Reid has found it convenient in his numerical work to put a short-range counter term in his potentials to cancel this highly singular repulsion and reduce the short-range behavior of the repulsion to r^{-1} . It is this counter term which makes the phenomenological potential strongly attractive at short ranges after the OPE term has been removed. It appears unlikely that the 3P_1 phase shift would be much affected if the behavior of the non-OPE potential within $0.4\mu_\pi^{-1}$ were repulsive rather than strongly attractive. It is therefore not necessarily significant that our theoretical potentials are also attractive at short ranges. Since the non-OPE potentials are small compared to the OPE potentials at both intermediate and long ranges, it is also unclear at this stage whether our potentials will move the phase shifts obtained from an OPE potential toward or away from the experimental phase shifts. We can only claim that the theoretical corrections to the OPE potential are small, in agreement with experiment.

3P_2 : Here we have qualitative agreement with Reid's phenomenological potentials again, insofar as the theoretical potentials have a short-range repulsion of about the same range. The theoretical potential does not have as strong an intermediate-range attraction, however. It is not clear to us at this stage exactly how sensitive to this intermediate-range attraction the phase shift will actually be. This is because the 3P_2 is coupled to the 3F_2 partial wave and, since it has a lower centrifugal barrier, will derive a strong effective intermediate-range attraction from this coupling. It may well be, therefore, that intermediate-range attraction in the diagonal ${}^3P_2 \rightarrow {}^3P_2$ potential may be traded off for a stronger off-diagonal ${}^3P_2 \rightarrow {}^3F_2$ potential. We turn now to this off-diagonal potential.

${}^3P_2 = {}^3F_2$: Here we find that Reid's phenomenological and our theoretical potentials are in *quantitative* agreement. We do not take this much more seriously than we would take qualitative agreement, however, because of the uncertainties in the calculation which are evident in the other potentials.

3F_2 : The comparison here is not too informative because the centrifugal barrier is already 250 MeV at an N - N separation of one-pion Compton wavelength. For this reason we have not considered potentials associated with other states which have $L \geq 3$.

1D_2 : Here there is reasonable agreement between theoretical and phenomenological potentials outside the comparison radius defined above. Inside the comparison radius it may be seen that the theoretical potential becomes strongly attractive. This strong attraction is not balanced off by a correspondingly large and singular OPE repulsion. Since the singular attrac-

tion increases more rapidly than r^{-2} at small r , it will be impossible to use this potential in a Schrödinger equation without modifying its short-range behavior. We conclude that our treatment, based as it is on one-boson exchange processes, must break down at small r . In this case, we find that at $0.2\mu_\pi^{-1}$ the vector-meson attraction of the two nucleons overcomes their centrifugal repulsion.

A comparison of our 1D_2 with our 1S_0 potentials shows that our theoretical potential is dependent upon $|\mathbf{L}|^2$. This term comes from the term in the vector-meson Born amplitude associated with the product of the small components of all four Dirac spinors. Such an $|\mathbf{L}|^2$ dependence has not appeared in previous theoretical potentials because these "small terms" in the Born amplitudes were neglected. We find that, although the coefficients of these terms are indeed small [of the order of $(M_\pi/2M)^4$, where M_π is the vector-meson mass], their dependence upon r is quite singular and they can therefore dominate the potentials at small r . Unfortunately the sign of our $|\mathbf{L}|^2$ term is in disagreement with that required by the experimental data, which indicate that the 1D_2 interaction is somewhat less attractive than the 1S_0 interaction.¹

3S_1 : Here again we are in qualitative agreement with Reid's phenomenological potential. The theoretical and phenomenological repulsive cores are in quite good agreement, but the theoretical intermediate-range attraction is considerably weaker than that present in Reid's phenomenological potential. Again there is some question here of how much of the intermediate-range attraction in the 3S_1 - 3S_1 diagonal potential can be traded off for the effective attraction due to the coupling to the 3D_1 channel. It may also be that the increased intermediate-range attraction required by Reid's potentials in both the 3S_1 and 1S_0 states indicates that the contribution due to the exchange of s -wave pion pairs is dynamically enhanced.

3S_1 - 3D_1 : Here there is good agreement between phenomenological and theoretical potentials. At $0.2\mu_\pi^{-1}$, the theoretical potential once again develops a very singular behavior, which will have to be suppressed if the theoretical potential is to be used in a coupled-channel Schrödinger equation.

3D_1 : Here again we have qualitative agreement with Reid's potential outside the comparison radius. Inside the comparison radius the two potentials diverge. This fact appears to have little significance, since a previous 3D_1 potential of Reid's, fitted to only slightly different experimental data, agreed quite well with our theoretical potential inside the comparison radius.

1P_1 : The N - N interaction in this partial wave shows an extraordinarily large repulsion in addition to the large OPE repulsion. There is also a strange long-range attraction which may simply reflect uncertainties in the n - p scattering data. We find a strong vector-meson repulsion and, for r greater than μ_π^{-1} , the vector-meson

repulsion and the coupled-channel attraction just about cancel each other.

3D_2 : Here again there is qualitative agreement between theoretical and phenomenological potentials.

Baryon-Baryon Repulsive Cores

In addition to the calculation of the N - N potential described above, we have calculated vector-meson-exchange potentials for all possible combinations of two baryons of the baryon octet.

Since single Λ 's and pairs of Λ 's are observed in hypernuclei, there is a considerable amount of interest in Λ - N and Λ - Λ interactions. Also, there has been speculation over the years concerning the possibility of strongly bound $I=\frac{3}{2}$ Σ - N and $I=1$ Ξ - N states which would be stable against strong interactions.

Our results have considerable relevance to these questions. From our calculation of the N - N potential we can say that the short-range repulsion due to vector-meson exchange in the 1S_0 and 3S_1 states accounts for the absence of strongly bound N - N states with binding energies of the order of 100 MeV. One might suppose, therefore, that, unless there are comparable repulsive cores in all the s -wave baryon-baryon systems listed above, some of them might possess strongly bound states.

In Fig. 2 we display the 1S_0 and 3S_1 vector-meson-exchange potentials in the various $SU(3)$ representations in which the baryon-baryon states fall. Symmetry breaking due to the mass splittings in the baryon octet and the vector-meson nonet has been neglected.

The average masses $M_B=1023.1$ MeV/ c^2 , $M_V=852.6$ MeV/ c^2 have been used.

In Fig. 3 are shown the projections of these vector-meson-exchange potentials onto the various physical states of current experimental interest. This projected potential $V_i(r)$ for the baryon-baryon system i is simply calculated as

$$V_i(r) = \sum_d |\langle i|d\rangle|^2 V_d(r),$$

where $d=1, 8_A, 8_S, 10, 10^*, 27$ are the various $SU(3)$ representations and the $\langle i|d\rangle$ symbolize the $SU(3)$ Clebsch-Gordon coefficients describing the amplitudes of the various $SU(3)$ representations in the states i . It can be seen that, because of the high statistical weight of the representations in which the vector-meson-exchange potential is repulsive, there are repulsive cores in almost all of the states of current experimental interest, and that these repulsive cores are comparable in strength to those in the N - N potentials (also drawn). This result is in accord with the experimental data on hypernuclei, which indicate the Λ - N and Λ - Λ attractions are too weak to produce a bound state, and it suggests that no *strongly* bound $T=\frac{3}{2}$ Σ - N will be found (none has yet been observed).

As the reader will see, the Ξ - N vector-meson-exchange potentials are exceptions to the rule of repulsive short-range behavior. Since a bound $I=0$ Ξ - N state is unstable to the strong decay $\Xi+N \rightarrow \Lambda+\Lambda+30$ MeV, we confine ourselves here to the question of the possible existence of a 1S_0 $I=1$ Ξ - N bound state which *would* be stable with respect to the strong interactions (the

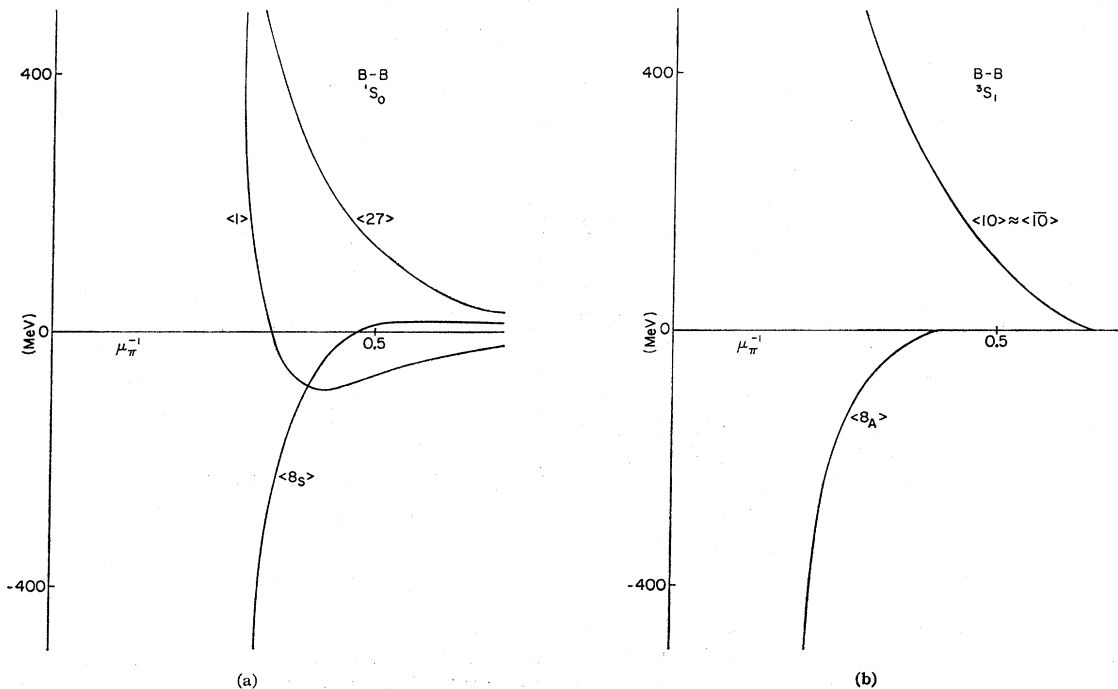


FIG. 2. Baryon-baryon vector-meson-exchange potentials in the $SU(3)$ -symmetry limit. Only the s -wave potentials are shown.

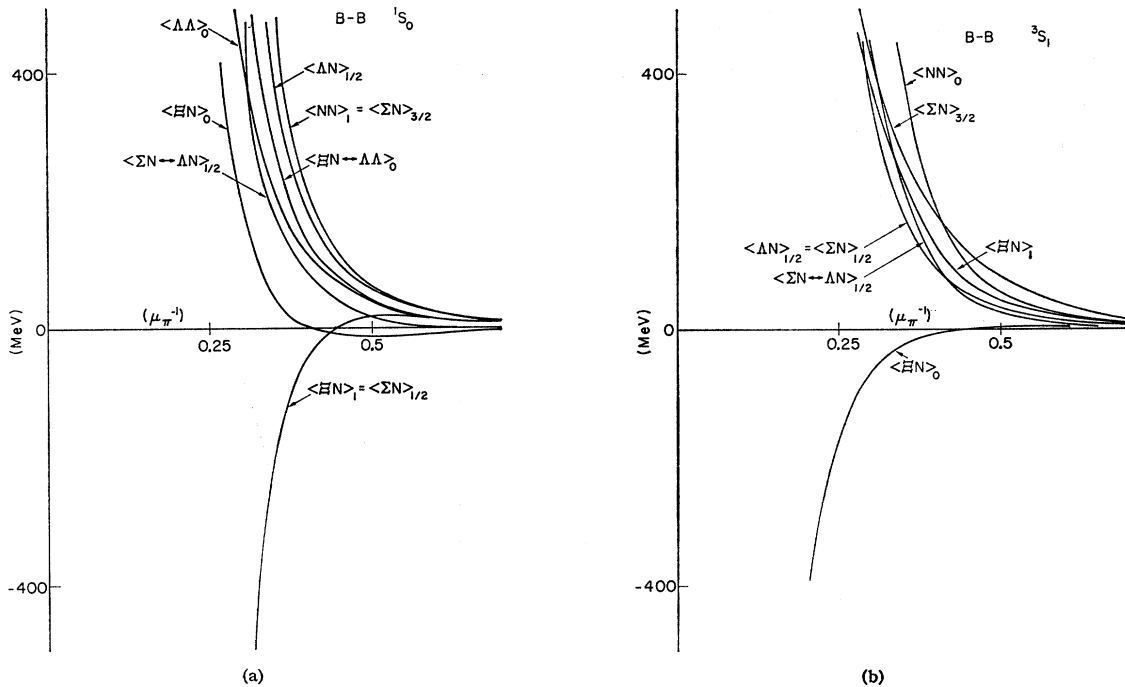


FIG. 3. The potentials of Fig. 2 projected onto the baryon-baryon states of practical interest.

neutral member of the triplet would be unstable with respect to the isospin-violating electromagnetic decay $\Xi + N \rightarrow \Lambda + \Lambda$.

If the $I=1$ 1S_0 Ξ - N interaction were as attractive at intermediate and long ranges as the N - N interaction in the s states, we could say with some confidence that there is a bound $I=1$ 1S_0 Ξ - N state. A strong intermediate-range attraction appears unlikely, however. Taking the d/f ratio of the pseudoscalar meson-baryon couplings to be $\frac{2}{3}$, we get a repulsive OPE potential in the Ξ - N s states with an absolute strength 0.04 of that of the attractive N - N OPE potential.

For the same d/f ratio, the effect of coupling of the Ξ - N to the Ξ - Δ (1236) and Ξ (1530)- N channels is reduced to 0.05 of the attractive effect which coupling to the N - Δ (1236) channel has on the N - N channel.

For these reasons we believe that the intermediate- and long-range Ξ - N potentials are likely to be considerably weaker than the corresponding parts of the N - N potentials; and an $I=1$ Ξ - N bound state, if it exists, will have to owe its binding energy to the short-range attractive vector-meson-exchange potential. Unfortunately, whether this potential is attractive enough to produce a bound state depends upon the behavior of the Ξ - N interaction inside $0.2\mu_\pi^{-1}$. Inside this radius our calculations are totally unreliable, and we therefore find that we cannot make a definite prediction as to whether or not an $I=1$ Ξ - N bound state exists. It appears likely that such a state would have escaped experimental detection.

Baryon-Antibaryon Attractive Core

Fermi and Yang⁸ considered the possibility that the pion might be a nucleon-antinucleon state bound by vector-meson exchange. The suggestion that there might be a large amplitude for the presence of a virtual baryon-antibaryon pair in the meson wave functions has been revived many times since. The short-range repulsion between baryons due to the $J^P=1^-$ vector-meson exchanges has been likened to the Coulomb repulsion between like charges due to $J^P=1^-$ photon exchange. The question naturally arises, therefore, as to whether these vector-meson-exchange potentials for B - \bar{B} interactions are strongly attractive in analogy with the Coulomb attraction between unlike charges.

We have found that the Coulomb analogy is deceptive in two respects. First, there are many terms in the vector-meson-exchange potential comparable in strength to the "Coulomb term."⁹ Therefore, an exact calculation of the B - \bar{B} vector-meson-exchange potential is necessary (contrary to our previous impression).¹⁰ Secondly, the idea of a universal repulsion between baryon pairs and a universal attraction between B - \bar{B} pairs is only as good as the approximation that the $SU(3)$ singlet vector-meson-exchange potential domi-

⁸ E. Fermi and C. N. Yang, Phys. Rev. 76, 1739 (1949).

⁹ By "Coulomb term" we mean the spin-independent term which remains in the static approximation. (In the static approximation the ratio of the mass of the vector meson to the mass of the baryon is taken equal to zero.)

¹⁰ H. Sugawara and F. von Hippel, Phys. Rev. 145, 1331 (1966).

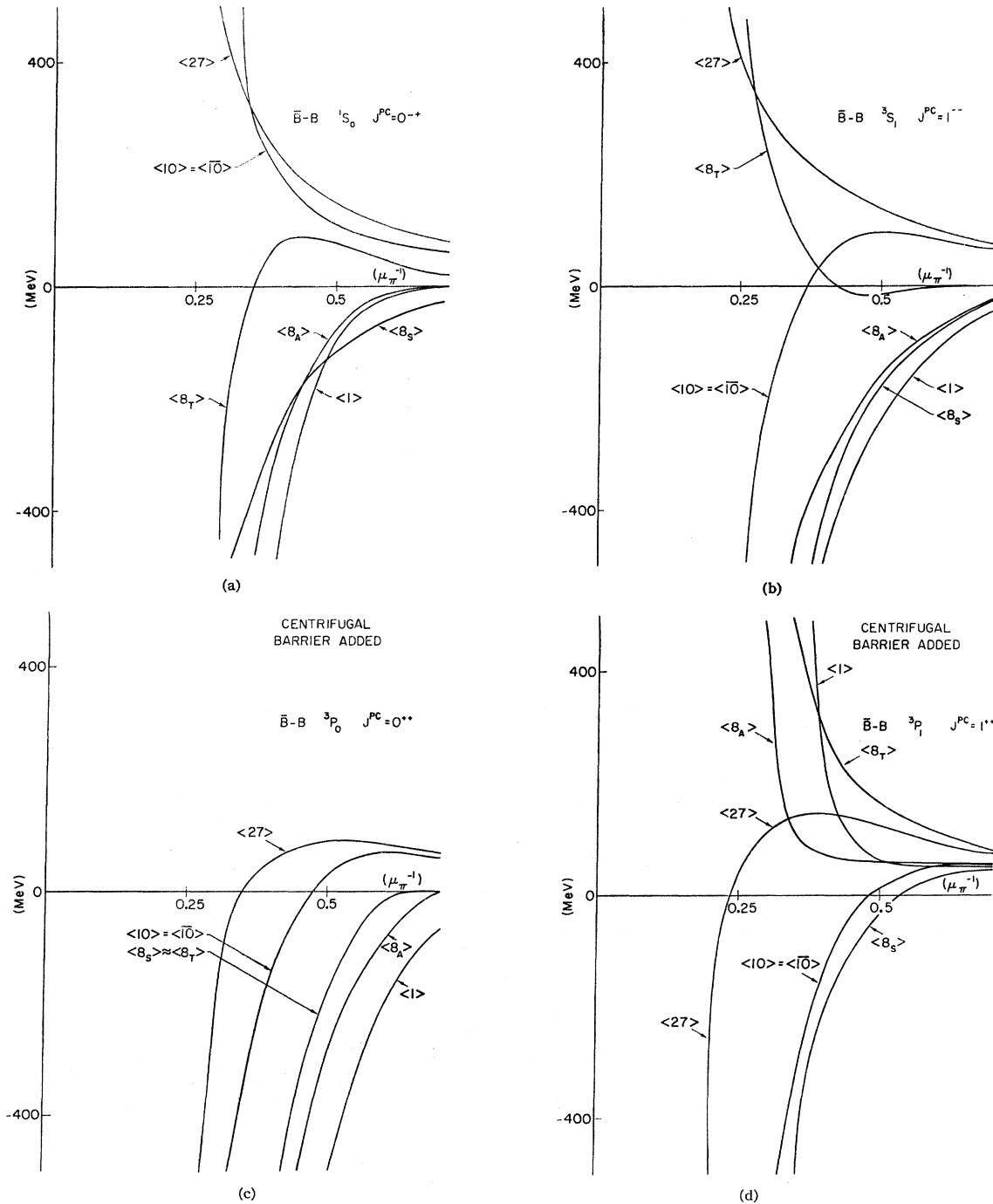


FIG. 4. Baryon-antibaryon vector-meson-exchange potentials in all $B\bar{B}$ states with $L=0, 1$. The states are labeled both spectroscopically, $(^{2S+1})L_J$, and by the quantum numbers used to classify bound states appearing as mesons.

nates potentials that are due to $SU(3)$ octet vector-meson exchange. If the octet-exchange potential is important, the potential will change sign for different isospin states or different hypercharge states because of ρ exchange or ω_8 exchange, etc.¹¹ We find, as can be seen from our results for the s -wave $B\bar{B}$ interaction discussed above, that the octet- and singlet-exchange

¹¹ J. Kalckar, Phys. Rev. **131**, 2242 (1963).

contributions are quite comparable, leading to attractive vector-meson-exchange potentials in some representations and repulsive vector-meson-exchange potentials in others. For the $B\bar{B}$ interactions, very interesting patterns of attractive and repulsive potentials develop.

In Fig. 4 we show our vector-meson-exchange potentials for all the $B\bar{B}$ states with $L=0, 1$. The curves shown are for an energy just above the elastic

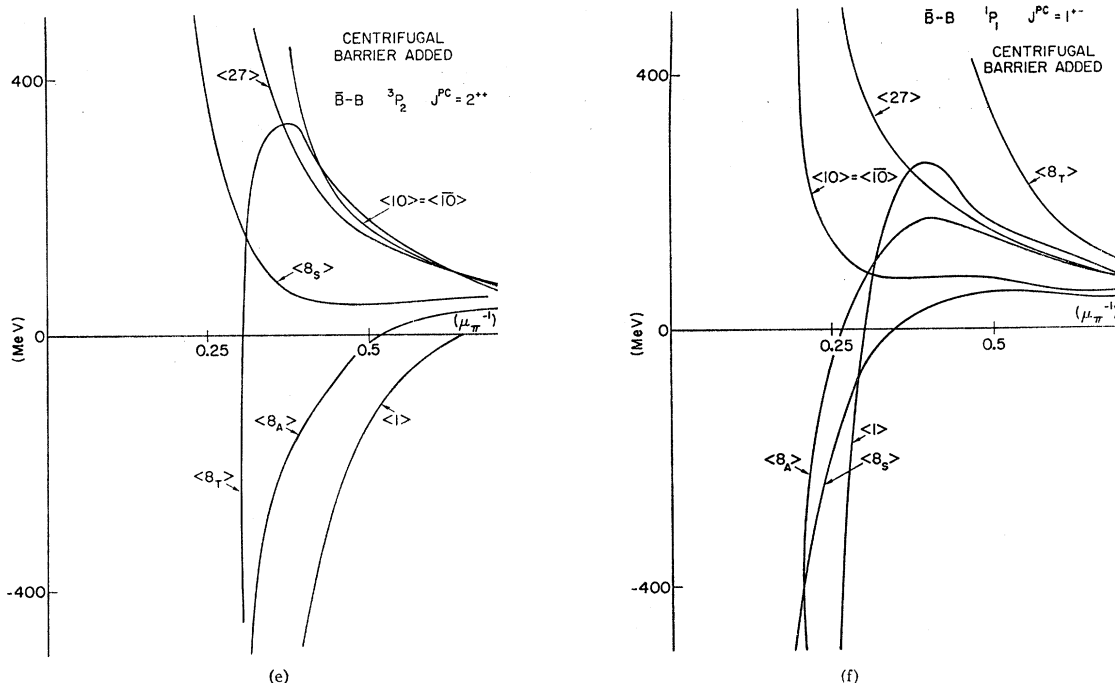


FIG. 4 (continued)

threshold and, as before, we have neglected all $SU(3)$ mass splittings.

In order to get an idea of the effectiveness of the vector-meson potential in $B\bar{B}$ states with nonzero orbital angular momentum, we have added to it the centrifugal repulsive barrier

$$V_L(r) = l(l+1)/Mr^2.$$

It will be seen that, generally, the attraction in $SU(3)$ singlets and octets is stronger than in other representations. Note also that there is a transition potential $\langle 8_T \rangle$ between the symmetric $\langle 8_S \rangle$ and antisymmetric $\langle 8_A \rangle$ octets.¹²

Where the $\langle 8_S \rangle$ and $\langle 8_A \rangle$ potentials are attractive enough to bind $B\bar{B}$ pairs in the corresponding $SU(3)$ representations, the effect of this transition potential will be to produce two mixed octets, one lying lower in mass than either the unmixed $\langle 8_S \rangle$ or $\langle 8_A \rangle$ and the other lying higher with the 10, 10^* , and 27. Thus we see that the tendency of the elastic vector-meson-exchange forces in the $\bar{B}B$ channel is to produce octets and singlets or nonets. Experimentally, no mesons have been established which cannot belong either to an $SU(3)$ octet or singlet.

The nonet pattern of the meson spectrum has been used to suggest an underlying $Q\bar{Q}$ structure of the mesons. We see here, as has been seen in many other calculations of the forces present in states with meson quantum numbers, that there may be a subtle pattern of the forces which leads to the same general results. It is of interest to note, therefore, that there *are* some

¹² This potential does not exist in the baryon-baryon interaction. It would violate Fermi-Dirac statistics.

divergences in the predictions of the two theories. In the case of the elastic $\bar{B}B$ interactions, we find that the nonet pattern is broken in the 3P_1 states (corresponding to $J^{PC} = 1^{++}$ mesons). The singlet interaction is repulsive and the decuplet interaction is weakly attractive. The 1^{++} mesons are not yet well enough established for us to be able to determine whether or not they do follow a nonet pattern.

Because the elastic $B\bar{B}$ forces play only one of the roles in the binding of the mesons, we do not devote any more time here to these results.

2. VECTOR-MESON-EXCHANGE CONTRIBUTIONS

Outline of the Calculation

In order to calculate the vector-meson potentials, we need to know the form and strength of the various vector-meson couplings to the baryons. Our best information on the form of the vector-meson coupling comes from the nucleon electromagnetic form factors. The rms radii of the charge and magnetic-moment distributions of the nucleons differ by only 20% from the radii which would be obtained if the ρ and ω mesons dominated the form factors. From the scaling laws of the nucleon form factors,¹³

$$\frac{F_M^p(q^2)}{F_E^p(q^2)} = \frac{\mu_p}{e}, \quad \frac{F_M^n(q^2)}{F_E^n(q^2)} = \frac{\mu_n}{\mu_p}, \quad \frac{F_E^n(q^2)}{F_E^p(q^2)} \approx 0, \quad (2.1)$$

we conclude that the electric and magnetic couplings

¹³ See, e.g., L. H. Chan, K. W. Chen, J. R. Dunning, Jr., N. F. Ramsey, J. K. Walker, and Richard Wilson, Phys. Rev. **141**, 1298 (1966).

of the vector mesons have simple $SU(3)$ transformation properties. We therefore use these couplings in our calculation rather than the conventional Dirac and Pauli couplings. Furthermore, we use the ratios of the proton-to-neutron electric and magnetic form factors to give us the F/D ratios of the vector-meson-octet electric and magnetic couplings and the ratio of the magnetic and electric form factors to fix the ratio of the corresponding couplings of the vector-meson octet.

Aside from our use of electric and magnetic couplings, all of these arguments, whereby the ratios of the vector-meson-baryon couplings are fixed by the nucleon form factors, are conventional. If all the vector mesons were members of an $SU(3)$ octet, it would only remain to fix the over-all strength of these couplings. In fact, however, the vector mesons form a nonet, i.e., there is an $SU(3)$ singlet vector meson present in addition to the octet. The electromagnetic form factors are no help in establishing the coupling strengths of the singlet since the photon couples only to the members of the octet.

At this point we call again on the experimentalists. It has been noted by several experimental groups that in the reactions

$$K^- + p \rightarrow \Lambda + (\phi \text{ or } \omega)$$

there is a substantial backward peak in the ω -production angular distribution and almost no backward ϕ production.¹⁴ If the backward peak in ω production is due to nucleon exchange, as seems likely, the absence of the backward peak in ϕ production indicates that the ϕ coupling to the nucleon is relatively much weaker. This fixes the relative strengths of the vector-meson octet and singlet couplings to the baryons. We have shown¹⁰ that this relationship is elegantly expressed in terms of the nonet formalism which Okubo¹⁵ has shown describes the $SU(3)$ tensor structure of the vector-meson nonet mass splittings and decay amplitudes. We have also shown¹⁰ that there is considerable indirect experimental evidence consistent with zero-strength ϕ couplings to the nucleons.

We have stated these arguments in $SU(3)$ language here because, in addition to the vector-meson-exchange contribution to the $N-N$ potential, we calculate the general $B-B$ and $B-\bar{B}$ interaction due to vector-meson exchange. For the coupling of the vector mesons at the $\bar{N}NV$ vertex, however, our estimates could be stated more simply: (a) The ϕ does not couple to the nucleon, and (b) the ω and ρ couplings are proportional to the isoscalar and isovector nucleon electromagnetic form factors, respectively.

Our remaining problem is to fix the over-all scale

¹⁴ G. W. London, R. R. Rau, N. P. Samios, S. S. Yamamoto, M. Goldberg, S. Lichtman, M. Primer, and J. Leitner, *Phys. Rev.* **143**, 1034 (1966); J. Badier, M. Demoulin, J. Goldberg, B. P. Gregory, C. Pelletier, A. Rouge, R. Barlontand, A. Derem, A. Leveque, J. Meyer, P. Schlein, A. Verglas, D. J. Holthuizen, W. Hoogland, J. C. Kluyver, and A. G. Tenner (Paris-Saclay-Amsterdam Collaboration), paper presented at The Oxford International Conference on Elementary Particles, 1965 (unpublished).

¹⁵ S. Okubo, *Phys. Letters* **5**, 165 (1963).

of the vector-meson couplings to the nucleons. It is difficult to do this reliably. As we shall discuss below, we believe that we can fix this scale to within a factor of 2 in the coupling constants squared. Fortunately, we find that this degree of uncertainty has little effect upon the qualitative behavior of our $N-N$ potentials. Although an uncertainty in the *relative* magnitudes of the vector-meson coupling constants could change the qualitative behavior of the $N-N$ potentials completely, a change in the absolute scale shifts the boundary of the region in which the vector-meson contributions dominate by only a few hundredths of a pion Compton wavelength. The reason is clear from Fig. 1; the vector-meson contributions to the potential decrease so rapidly as a function of r that the interval over which they change by a factor of 2 is quite small. Only the range of these contributions is important, because they are so repulsive.

Once all of the vector-meson coupling constants have been fixed by the above arguments, our procedure is quite straightforward. We calculate the one-vector-meson-exchange Born amplitudes for $N-N$, $B-B$, or $\bar{B}-B$ scattering and then Fourier-transform these Born amplitudes to obtain an energy-dependent potential which in Born approximation gives back the original Born amplitude. Uncertainties which arise in the translation of Born amplitudes to potentials are discussed at the end of this section.

$SU(3)$ Structure of Vector-Meson Couplings to the Baryons

The $SU(3)$ structure of our vector-meson-baryon couplings is most easily understood if the members of the baryon octet are represented by three quark tensor wave functions of mixed symmetry and the members of the vector-meson nonet by $Q-\bar{Q}$ tensor wave functions. The mathematical quark composition of each of the baryons may be represented in the matrix superposition of all of the eight baryon wave functions shown below¹⁶:

$$B_8^{ij,k} = \sum_{\alpha=1}^8 b_{\alpha}^{ij,k},$$

$$B_8^{ij,1} = \begin{pmatrix} 0 & -P/\sqrt{2} & -\Sigma^+/\sqrt{2} \\ P/\sqrt{2} & 0 & \frac{1}{2}\Sigma^0 + \Lambda^0/\sqrt{12} \\ \Sigma^+/\sqrt{2} & -\frac{1}{2}\Sigma^0 - \Lambda^0/\sqrt{12} & 0 \end{pmatrix},$$

$$B_8^{ij,2} = \begin{pmatrix} 0 & -n/\sqrt{2} & \frac{1}{2}\Sigma^0 - \Lambda^0/\sqrt{12} \\ n/\sqrt{2} & 0 & \Sigma^-/\sqrt{2} \\ -\frac{1}{2}\Sigma^0 + \Lambda^0/\sqrt{12} & -\Sigma^-/\sqrt{2} & 0 \end{pmatrix},$$

$$B_8^{ij,3} = \begin{pmatrix} 0 & -\Lambda^0/\sqrt{3} & \Xi^0/\sqrt{2} \\ \Lambda^0/\sqrt{3} & 0 & \Xi^-/\sqrt{2} \\ -\Xi^0/\sqrt{2} & -\Xi^-/\sqrt{2} & 0 \end{pmatrix}.$$

The vector-meson wave functions, in terms of their $Q-\bar{Q}$ composition, may be represented by the super-

¹⁶ M. Gell-Mann, *Phys. Letters* **8**, 214 (1964); G. Zweig, CERN Report No. 8419/TH412, 1964 (unpublished).

position

$$(V_9)^i_j = \sum_{a=1}^9 (v_a)^i_j,$$

$$(V_9)^i_j = q^i q^j = \begin{bmatrix} \rho^0/\sqrt{2} + \omega_8/\sqrt{6} + \omega_1/\sqrt{3} & \rho^+ & K^{*+} \\ \rho^- & -\rho^0/\sqrt{2} + \omega_8/\sqrt{6} + \omega_1/\sqrt{3} & K^{*0} \\ K^{*-} & \bar{K}^{*0} & -(2/\sqrt{6})\omega_8 + \omega_1/\sqrt{3} \end{bmatrix}, \quad (2.3)$$

where the last matrix takes into account the approximate mixtures of the singlet and octet mesons present in the ω and ϕ^{15} ;

$$\begin{aligned} \omega &\approx (\sqrt{\frac{2}{3}})\omega_1 + (\sqrt{\frac{1}{3}})\omega_8, \\ \phi &\approx -(\sqrt{\frac{1}{3}})\omega_1 + (\sqrt{\frac{2}{3}})\omega_8. \end{aligned} \quad (2.4)$$

The relative strength g^{abc} of the coupling of a vector meson V_b to a baryon vertex $\bar{B}_a B_c$ including nonet constraints may be obtained through a contraction of quark with antiquark indices in a product of these wave functions,^{10,17}

$$g^{abc}(f, d) = b_{ij, k^a}(v_b)^k b_c^{ij, l} + 2(f-d)b_{ij, k^a}(v_b)^k b_c^{ij, k}, \quad (2.5)$$

where f and d are proportional to the F -type and D -type coupling constants, respectively, with $f+d=1$.

Below we use the ratios of the observed electromagnetic nucleon form factors to fix the constants f and d and the spin structure of the vector-meson couplings. Because the mass associated with the electromagnetic form factor slopes at $q^2=0$ differs by only 20% from the ρ and ω masses, we expect that the spin structure of the electromagnetic couplings and the F/D ratios of these couplings should be closely related to those of the vector mesons.

If spin structure of the electromagnetic vertex is analyzed into a sum of electric and magnetic couplings rather than into a sum of the conventional Dirac and Pauli couplings, the corresponding experimental neutron and proton form factors are found to be in the constant ratios [Eq. (2.1)] as a function of q^2 .¹⁸ In other words, for this choice of spin structure of the nucleon-photon couplings, the F/D ratios for each of the electric and magnetic vertices are constant as a function of q^2 .

The vector-meson contributions to the form-factor spectral functions will have this effect only if there are definite F/D ratios for the electric and magnetic couplings of the vector mesons to the nucleons.¹⁸ If the vector-meson couplings have this property of the

¹⁷ The most general possible $SU(3)$ -invariant coupling can be obtained from (2.4) by adding term $g_s b_{ij, k^a} b_c^{ij, k}(v_b)^k$. Because all vector-meson wave functions are traceless, aside from the $SU(3)$ singlet, this term corresponds to an extra independent coupling for the singlet meson. The experimental observation $(g_N \bar{N}_a)^2 / (g_N \bar{N}_\omega)^2 \approx 0$ fixes $g_s \approx 0$.

¹⁸ The coupling constants to the proton of those vector mesons which can contribute to the electromagnetic form-factor spectral functions are, according to (2.4), $g_\rho = (f+d)/\sqrt{2}$, $g_\omega = (3f-d)/\sqrt{2}$, $g_\phi = 0$. Because of the degeneracy of the ρ and ω masses and the decoupling of the ϕ , the mass splittings of the vector mesons do not break the proportionalities (2.1).

experimental form factors, we must construct the $\bar{B}_a B_c V_b$ vertex as

$$\Gamma_{abc} = \langle a | J_\nu^b | c \rangle V_b^\nu, \quad (2.6a)$$

where^{19,20}

$$\begin{aligned} \langle a | J_\nu^b | c \rangle &= G_E g^{abc}(f_E, d_E) \bar{u}(\mathbf{P}_a S_a) \frac{P_\nu}{2M} u(\mathbf{P}_c S_c) \\ &\quad - i G_M g^{abc}(f_M, d_M) \bar{u}(\mathbf{P}_a S_a) \gamma_5 \epsilon_{\kappa\lambda\mu\nu} \frac{P^\kappa q^\lambda}{4M^2} \gamma^{\mu\nu} u(\mathbf{P}_c S_c) \end{aligned} \quad (2.6b)$$

and

$$P_\nu = (p_a + p_c)_\nu, \quad q_\nu = (p_a - p_c)_\nu.$$

The coupling constants $g^{abc}(f_E, d_E)$, $g^{abc}(f_M, d_M)$ are obtained as indicated in Eq. (2.5). The D/F ratios for the electric and magnetic couplings are fixed by the ratios of the corresponding proton and neutron form factors in (2.1) and the assumption that the photon couples through the superposition of vector mesons, which transforms as the $SU(3)$ charge generator Q ,

$$\gamma \rightarrow V_Q, \quad V_Q \propto \text{Tr}(Q V_a) = \rho^0/\sqrt{2} + \omega/3\sqrt{2} + \frac{1}{3}\phi,$$

where

$$Q = \begin{bmatrix} \frac{2}{3} & 0 & 0 \\ 0 & -\frac{1}{3} & 0 \\ 0 & 0 & -\frac{1}{3} \end{bmatrix}.$$

We obtain

$$d_E/f_E = 0, \quad d_M/f_M = \frac{3}{2}. \quad (2.6c)$$

The relative magnitudes of the electric and magnetic couplings G_E/G_M have been fixed in the same way by the ratio of the proton electric and magnetic form factors, giving

$$G_M/G_E = (5/3)(2M\mu_p)/e = (5/13)2.79. \quad (2.6d)$$

Finally, it is necessary to fix the over-all scale of the coupling constants.

Scale of Vector-Meson Couplings

A variety of estimates, all rough, may be made. We discuss here the conventional estimates in terms of the

¹⁹ Our conventions for γ matrices are those of J. D. Bjorken and S. D. Drell, *Relativistic Quantum Fields* (McGraw-Hill Book Company, New York, 1965).

²⁰ For those not familiar with these couplings, Eq. (2.6b) may be seen to have the static limit

$$\begin{aligned} j_\nu^b V_b^\nu &\xrightarrow{p_a, p_c \rightarrow 0} G_E g^{abc}(f_E, d_E) [\chi_a^\dagger \chi_c] V_b^0 \\ &\quad - i G_M g^{abc}(f_M, d_M) [\chi_a^\dagger (\boldsymbol{\sigma} \times \mathbf{q}/2M) \chi_c] \cdot \mathbf{V}_b, \end{aligned}$$

where the electric and magnetic character of the two couplings becomes obvious.

electric ρ^0 coupling constant to the proton g_ρ^E to which all the others may be normalized.

From Partial-Wave Dispersion Relations

The ρ Dirac coupling constant has been estimated by Hamilton and co-workers²¹ in a phenomenological treatment of the contribution of ρ exchange to the π - N partial-wave amplitudes. From this and the relationships between the vector coupling constants on the vector-meson mass shell, we obtain a value of²²

$$(g_\rho^E)^2/4\pi \approx 1.8$$

for the ρ . Hamilton *et al.* have made this estimate, however, by assuming that the ratio of the Pauli and Dirac coupling constants of the ρ^0 on its mass shell is equal to that of the corresponding isovector form factors at $q^2=0$. We have argued above that it is the ratio of the *electric* and *magnetic* coupling constants of the ρ on its mass shell that is equal to the ratio of the corresponding isovector form factors at $q^2=0$. Our assumption would imply that the ratio of Pauli to Dirac coupling constants of the ρ on its mass shell,

$$f_{\bar{p}p\rho^0}^P/f_{\bar{p}p\rho^0}^D \approx 15.6,$$

is considerably larger than that assumed by Hamilton *et al.*,

$$f_{\bar{p}p\rho^0}^P/f_{\bar{p}p\rho^0}^D = \mu_V/e_V \approx 3.6.$$

Upon examination of the expressions of Hamilton *et al.*, it appears that their results for $f_{\bar{p}p\rho^0}^D$ are very sensitive to the assumed ratio of f^P/f^D . The value of $(g_{\bar{p}p\rho^0}^E)^2/4\pi$ quoted above is therefore not correct and should probably be reduced.

Pole-Dominance Model of the Form Factors

Another estimate of the ρ meson couplings to the nucleon is obtained from a ρ^0 pole approximation to the isovector nucleon electromagnetic form factors.²³ In such an approximation to the isovector electric form factor, the isovector nucleon charge $\frac{1}{2}e$ is given by the simple expression

$$\frac{1}{2}e = g_\rho^E \gamma_\rho / M_\rho^2, \quad (2.7)$$

where γ_ρ is the ρ -photon coupling constant and M_ρ is the ρ mass. Thus, if the coupling of the ρ to the photon is known, g_ρ^E may be estimated from Eq. (2.7).

²¹ See, e.g., A. Donnachie, J. Hamilton, and A. T. Lea, *Phys. Rev.* **135**, B515 (1964), where earlier references may be found.

²² To avoid confusion, it should be pointed out that normally the ρ coupling constant is defined as *twice* the $\bar{p}p\rho^0$ coupling constant. Therefore our values of $(g_\rho^E)^2/4\pi$ will appear to be about four times too small to the reader familiar with the literature [see, e.g., J. J. Sakurai, *Phys. Rev. Letters* **17**, 1021 (1966)].

²³ We shall discuss the effect on our estimates of corrections to pole dominance below. We have already used a weaker form of this approximation in our assumption that the ρ - N coupling constants are in the proportion of the isovector form factors.

The most direct way to determine γ_ρ is to measure the decay rate

$$\rho \rightarrow l^+ + l^- \quad (e^+ + e^- \text{ or } \mu^+ + \mu^-).$$

Recently, three measurements of the branching ratio

$$\Gamma_l/\Gamma_\pi = (\rho^0 \rightarrow l^+ + l^-)/(\rho^0 \rightarrow \pi^+ + \pi^-)$$

have been made, with the result

$$\Gamma_l/\Gamma_\pi = (5.1_{-0.7}^{+1.6}) \times 10^{-5},^{24} \quad (5.1 \pm 1.2) \times 10^{-5},^{25} \\ (5.7 \pm 0.7) \times 10^{-5}.^{26}$$

Using the branching ratio $(5.5 \pm 0.5) \times 10^{-5}$ and the value²⁷

$$\Gamma(\rho^0 \rightarrow \pi^+ + \pi^-) = 140 \text{ MeV},$$

we obtain the absolute ρ^0 leptonic decay ratio which gives,²⁸ in turn, the ρ - γ coupling constant that we can use in Eq. (2.7) to give us the estimate $(g_\rho^E)^2/4\pi = 0.5$.

This estimate is based upon the assumption of complete ρ dominance of the isovector nucleon form factors—an assumption which is not valid experimentally. Although it is impossible to estimate quantitatively the corrections to this estimate without a model for the other contributions to the isovector form factors, one may say the following: The rapid decrease of the form factors¹³ at large q^2 requires that the other contributions to the isovector form-factor spectral functions have a net opposite sign to the sign of the ρ^0 pole residue. This means that their contributions to the isovector charge will tend to cancel the ρ^0 contribution and that, to maintain the $q^2=0$ values of the form factors, the ρ - N coupling must be increased above the estimates made above on the basis of the ρ^0 -dominance model.

The value of $(g_\rho^E)^2/4\pi$ that we have actually used in our calculations is

$$(g_\rho^E)^2/4\pi \approx 1.$$

This is our best guess in view of the uncertainties discussed above, and it seems unlikely that the actual value of $(g_\rho^E)^2$ will differ from this estimate by more than a factor of 2. It should be emphasized once again that only our determination of the over-all scale of the vector-meson coupling constants is directly related to the validity of the vector-dominance assumption. As

²⁴ J. K. de Pagter, J. I. Friedman, G. Glass, R. C. Chase, M. Gettner, E. von Goeler, Roy Weinstein, and A. Boyarski, *Phys. Rev. Letters* **16**, 35 (1966); see also R. Weinstein, in *Proceedings of the Thirteenth International Conference on High-Energy Physics* (University of California Press, Berkeley, 1967), p. 99.

²⁵ A. Weyman, E. Engels, Jr., L. N. Hand, C. M. Hoffman, P. G. Innocenti, Richard Wilson, W. A. Blanpied, D. J. Drickey, and D. G. Stairs, *Phys. Rev. Letters* **17**, 1113 (1966); **18**, 929 (1967).

²⁶ J. G. Asbury, U. Becker, W. K. Bertram, P. Joos, M. Rohde, A. J. S. Smith, C. L. Jordan, and S. C. C. Ting, *Phys. Rev. Letters* **19**, 869 (1967).

²⁷ A. H. Rosenfeld, A. Barbaro-Galtieri, W. J. Podolsky, L. R. Price, P. Soding, C. G. Wohl, M. Roos, and W. J. Willis, *Rev. Mod. Phys.* **39**, 1 (1967).

²⁸ Y. Nambu and J. J. Sakurai, *Phys. Rev. Letters* **8**, 79 (1962).

has been stated above, an over-all uncertainty in the scale of the vector-meson-exchange potential does not materially affect our qualitative results.

Translation of Born Amplitudes into Potentials

The N - N interaction is conventionally described by theoretical or phenomenological potentials. This is because the Schrödinger equation is employed in most discussions of the properties of nuclei. We have therefore translated our vector-meson-exchange Born amplitudes into corresponding potentials.

The standard procedure for translating a Born scattering amplitude for a particular isospin state into a nonrelativistic potential may be summarized as follows (see also Appendix A): The Born amplitude is rewritten as a function of the variables E , \mathbf{q} , \mathbf{P} , where E is the energy and \mathbf{P} and \mathbf{q} are, respectively, the sum and difference of the final and initial 3-momenta of one of the nucleons in the c.m. system. All Dirac spinor contractions are then reexpressed in terms of sums of Pauli spinor contractions and all \mathbf{q} dependence is Fourier-transformed into \mathbf{r} dependence. The result may be expressed as

$$\begin{aligned} [V(\mathbf{P}, \mathbf{r}, E)]_{\alpha'\beta', \alpha\beta} = & V_C(\mathbf{r}, E)\delta_{\alpha'\alpha}\delta_{\beta'\beta} \\ & + V_\sigma(\mathbf{r}, E)\sigma_{\alpha'\alpha} \cdot \sigma_{\beta'\beta} + V_T(\mathbf{r}, E)[S_{12}]_{\alpha'\beta', \alpha\beta} \\ & + V_{LS}(\mathbf{r}, E)\left[\frac{1}{2}\sigma_{\alpha'\alpha}\delta_{\beta'\beta} + \frac{1}{2}\delta_{\alpha'\alpha}\sigma_{\beta'\beta}\right] \cdot (\mathbf{r} \times \mathbf{P}) \\ & + V_{LS_2}(\mathbf{r}, E)[\sigma_{\alpha'\alpha} \cdot (\mathbf{r} \times \mathbf{P})][\sigma_{\beta'\beta} \cdot (\mathbf{r} \times \mathbf{P})] \\ & + V_{P_2}(\mathbf{r}, E)[(\sigma_{\alpha'\alpha} \times \mathbf{P}) \cdot (\sigma_{\beta'\beta} \times \mathbf{P})]. \quad (2.8) \end{aligned}$$

The functions $V(\mathbf{r}, E)$ are sums of Yukawa functions, δ functions, and their derivatives, multiplied by simple rational functions of E .

The usual approximations²⁹ on this result are to set $E=M$ and neglect the last two terms which are due to the "small" components of all four Dirac spinors. We have not made these approximations because they would result in the vector-meson-exchange potentials making a negligible contribution to the N - N s -wave potentials.

The reason for this is a cancellation between the two terms which contribute to the s -wave potentials in this approximation,

$$\left(\frac{e_1 e_2}{4\pi}\right) \frac{\exp(-M_V r)}{r} + \left(\frac{\mu_1 \mu_2}{4\pi}\right) \left(\frac{M_V}{2M}\right)^2 \sigma_1 \cdot \sigma_2 \frac{\exp(-M_V r)}{r}.$$

(The first term in this expression represents the "electric" interaction of the nucleons through the non-spin-flip vector-meson couplings, while the second term represents the effect of the "magnetic" or spin-flip vector-meson interaction. The symbolic coupling-constant products $e_1 e_2$, $\mu_1 \mu_2$ represent the effect of summing over the various exchanged mesons and M , M_V represent the nucleon and average vector-meson

²⁹ See, e.g., R. A. Bryan and B. L. Scott, Phys. Rev. **135**, B434 (1964).

masses, respectively.) Because these terms cancel so completely, we have had to calculate a more accurate vector-meson-exchange potential, i.e., one which will give back the exact relativistic Born amplitude in Born approximation.

There is no difficulty in dropping the approximation $E=M$. This just results in our potentials developing a weak energy dependence, as indicated by the argument E in coefficient potentials of Eq. (2.8). The difficulty arises with the last two terms of Eq. (2.8). Although the fourth term can be translated into an $\mathbf{L} \cdot \mathbf{S}$ operator which is diagonal with respect to the basis $|JLS\rangle$, the fifth term can only be partially diagonalized in terms of $|\mathbf{L}|^2$, $(\mathbf{L} \cdot \mathbf{S})^2$, and $\mathbf{L} \cdot \mathbf{S}$, and the sixth term cannot even be partially diagonalized in such a simple manner.

In Appendix A we discuss the manipulations and approximations by which we have reduced the last two terms in Eq. (2.8) to potentials of the standard form of the first four terms plus an additional term

$$V_Q(\mathbf{r}, E)Q_{12},$$

where

$$Q_{12} = \frac{1}{2}[(\mathbf{L} \cdot \sigma_1)(\mathbf{L} \cdot \sigma_2) + (\mathbf{L} \cdot \sigma_2)(\mathbf{L} \cdot \sigma_1)]. \quad (2.9)$$

The final forms have some explicit dependences of the coefficient potentials $V_i(\mathbf{r}, E)$ on $|\mathbf{L}|^2$.

It is well known that such a reduction procedure is not unique; different energy-dependent potentials will give rise to the same Born amplitude. It should be pointed out, however, that the "unconventional" terms obtained from the last two terms of Eq. (2.8) only play an important role in our s -wave potentials and give remarkably good results there.

3. COUPLED-CHANNEL CONTRIBUTIONS

After completing the zero-parameter calculation of the vector-meson-exchange potentials discussed in Sec. 2, we combined them with the OPE potential and compared the sum with Reid's phenomenological potentials. Although we found qualitative agreement for $r < 0.5$ F and for $r > 1.5$ F, the phenomenological potentials were found to have considerably more intermediate-range attraction in almost all states.

An inability to reproduce this intermediate-range attraction is a malady which has afflicted one-boson-exchange models even when the vector-meson coupling constants have been taken as adjustable parameters. For this reason, and because we get such good results for small r , we do not interpret the discrepancy as indicating an error in our choice of vector-meson coupling constants. Instead we conclude that there is another contribution to the N - N potential which must be taken into account.

The range of this contribution suggests the exchange of a system whose mass lies between the masses of the vector mesons and the pion. Models involving the

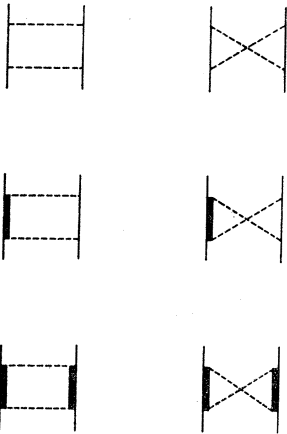


FIG. 5. Two-pion-exchange contributions considered by ALV (Ref. 31).

exchange of a light scalar meson, two interacting pions, or two uncorrelated pions have been proposed.

Scalar-Meson Model

In most recent models, the intermediate-range attraction has been obtained by assuming the exchange of an unknown $I=0$ scalar meson and adjusting its mass and coupling constant to obtain the best fit to the experimental data.³⁰

The likelihood of a reasonably narrow low-mass resonance having remained undetected till now steadily diminishes, but it has been pointed out³⁰ that a strong nonresonant $\pi\text{-}\pi$ attraction in the $I=0$ state might enhance the exchange of $I=0$ s -wave pion pairs enough to simulate the effect of a scalar-meson exchange. The net result is the same; our ignorance is expressed by adjustable parameters.

Two-Pion-Exchange Model

In the older models of the $N\text{-}N$ interaction, the intermediate-range attraction was attributed to the exchange of two pions. Most recently Amati, Leader, and Vitale (ALV)³¹ pointed out that the two-pion-exchange contribution to $N\text{-}N$ scattering corresponds to the contribution of the inelastic reaction $N+N \rightarrow \pi+\pi$ through unitarity in the crossed channels of the $N\text{-}N$ scattering amplitude. The reaction

$$N+\bar{N} \rightarrow \pi+\pi$$

is, in turn, simply the analytic continuation into *its* crossed channel of $\pi\text{-}N$ scattering. Consequently, if a good model of the $\pi\text{-}N$ scattering amplitude were available, and its continuation into the crossed channel could be relied upon, it would be possible to calculate the two-pion-exchange contribution to the $N\text{-}N$ interaction.

³⁰ See, e.g., A. Scotti and D. Y. Wong, Phys. Rev. **138B**, 145 (1965); R. A. Bryan and R. A. Arndt, *ibid.* **150**, 1299 (1966).

³¹ D. Amati, E. Leader, and B. Vitale, Nuovo Cimento **17**, 68 (1960); **18**, 409 (1960); Phys. Rev. **130**, 750 (1963); see also W. N. Cottingham and R. Mau, *ibid.* **130**, 735 (1963).

ALV approximated the $\pi\text{-}N$ scattering amplitude by the direct and crossed nucleon and $\Delta(1236)$ poles.³² They added ρ exchange and, following Bowcock, Cottingham, and Lurié (BCL),³³ arbitrary constants whose values were adjusted to give the experimental s -wave scattering lengths.

Unfortunately this model of $\pi\text{-}N$ scattering is still not very satisfactory. Durso has shown³⁴ that it is the amplitude for exchanging a low-energy pion pair in a relative s state that gives the dominant contribution to the ALV result. As he points out, the BCL model is at its weakest in describing this amplitude. It appears that a more sophisticated treatment of $\pi\text{-}N$ scattering will be necessary if the $N\text{-}N$ two-pion-exchange interaction is to be calculated in a convincing manner.

Coupled-Channel Model

We do not propose to make these improvements here. Rather, we wish to clarify some of the basic physics involved in the ALV approach. Our idea is that the intermediate-range attraction can be more easily understood as the effect of inelastic interactions in the s channel rather than in the t channel. From this point of view we are coupling a lower channel to a higher channel, which, as is well known in quantum mechanics, results in an added attraction in the lower channel (see Fig. 5).³⁵ The particular higher channels, whose effects we believe we can calculate rather reliably, are the $N\text{-}\Delta(1236)$ and $\Delta(1236)\text{-}\Delta(1236)$ channels.

In a dispersion-theory approach, coupling to these channels would result in important inelastic cuts in the $N\text{-}N$ scattering amplitude. [Experimentally, single $\Delta(1236)$ production dominates the inelastic $N\text{-}N$ cross section over a considerable range of energies above threshold.³⁶ Although double $\Delta(1236)$ production is less important experimentally,³⁷ we find that it also gives important contributions to the $N\text{-}N$ intermediate-

³² This is the so-called CGLN approximation [G. F. Chew, M. L. Goldberger, F. Low, and Y. Nambu, Phys. Rev. **106**, 1337 (1957)].

³³ J. Bowcock, W. N. Cottingham, and D. Lurié, Phys. Rev. Letters **5**, 386 (1960).

³⁴ J. W. Durso, Phys. Rev. **149**, 1234 (1966).

³⁵ The ALV calculation considered the two-pion-exchange diagrams shown in Fig. 5. The various two-pion-exchange box diagrams may be seen to contain, respectively, two nucleons, a nucleon and a $\Delta(1236)$, and two $\Delta(1236)$'s both with and without a pion pair in the intermediate inelastic channel. We neglect here the contributions corresponding to the crossed box diagrams. Furthermore, we will assume that most of the effect of the diagram with two nucleons in the intermediate state is contained in the iteration of the OPE potential in the solution of the Schrödinger equation. Finally, we employ nonrelativistic approximations in order to obtain an estimate of the effect of the remaining box diagrams containing $\Delta(1236)\text{-}N$ and $\Delta(1236)\text{-}\Delta(1236)$ intermediate states. The advantage will be seen in the ease with which "unitarity suppression" of reactions II and III at small impact parameters may be taken into account within the nonrelativistic framework.

³⁶ At 400, 600, 800, and 1100 MeV proton-proton c.m. kinetic energy, the production cross section is 22.1 out of 22.6 mb, 18.9 out of 26.6 mb, 16.3 out of 27 mb, and 7.3 out of 27 mb, respectively. (See Ref. 4.)

range attraction,³⁸ especially in the $I=0$ states which do not couple to the $N\text{-}\Delta(1236)$ channel.]

Our basic approach is nonrelativistic: Consider the wave function in the relative coordinate of two physical nucleons for a continuum state below all inelastic thresholds. We will assume that the two nucleons are in an eigenstate of isospin, total angular momentum, and parity, with the corresponding quantum numbers (I, J, P) . Because all inelastic channels are closed, the amplitude for finding any state other than a free $N\text{-}N$ state must go to zero exponentially for large separations.

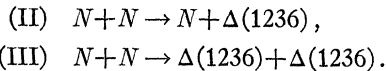
Within the region of interaction, however, there will be a nonzero amplitude for finding the virtual excited states of the $N\text{-}N$ system. Our purpose here is to estimate the effect on the elastic $N\text{-}N$ interaction of what we believe may be the most important virtual excited states present: the two-body $N\text{-}\Delta(1236)$ and $\Delta(1236)\text{-}\Delta(1236)$ states.

For our estimates we use a framework within which we treat the $N\text{-}N$, $N\text{-}\Delta(1236)$, and $\Delta(1236)\text{-}\Delta(1236)$ states as the three channels of a coupled-channel Schrödinger equation. [We have neglected the width of the $\Delta(1236)$ in these calculations so as to be able to treat all of these states on the same basis as genuine two-particle states.] We do not solve the Schrödinger equation but merely use it as a vehicle for a completeness approximation calculation.

In our three-channel Schrödinger equation we have a matrix of potentials: transition potentials connecting pairs of channels, and diagonal potentials associated with a single channel.

Potentials

We calculate the transition potentials between the $N\text{-}N$ and virtual $N\text{-}\Delta(1236)$ and $\Delta(1236)\text{-}\Delta(1236)$ states from a modified OPE model for the inelastic reactions³



In Appendix B we present our calculations of the ordinary OPE Born amplitudes for these reactions. We then drop some small terms in the amplitudes in order to avoid doing a more complicated calculation

³⁷ It has been estimated to represent 1.8 mb cross section at 500 MeV $p\text{-}p$ c.m. kinetic energy and 4.1 mb at 800 MeV $p\text{-}p$ c.m. kinetic energy. (See Ref. 6.)

³⁸ The reason for the relatively small double $\Delta(1236)$ production cross section may be understood semiclassically: The semiclassical $N\text{-}N$ impact parameter equals L/k , where L is the orbital angular momentum and k is the c.m. momentum of one of the nucleons. In the $\Delta(1236)\text{-}\Delta(1236)$ channel, the impact parameter is L^*/k^* , where L^* and k^* are the corresponding quantities in this channel. If k^* is much less than k , as it is in this case, then, semiclassically, L should be much less than L^* . The difference cannot be greater than $|L-L^*|=2$; therefore, the wave function overlap will be rather poor. It is obvious that this argument does not apply to virtual transitions where we may have $k^* \approx k$. Therefore the effect of the coupling of the $N\text{-}N$ channel to channel III may be comparable to that due to the coupling to channel II (as we find it to be).

than our present state of sophistication would warrant. We also evaluate the Fourier transforms of the amplitudes. These Fourier transforms are the OPE transition potentials. The Born approximation to these potentials would give back the original Born amplitude except for subtraction terms associated with δ functions and derivatives of δ -function potentials at the origin which we have ignored.

It is well known, however, that unmodified OPE amplitudes do not describe the experimental data in reactions such as II and III at all well. Recently, it has been shown, within the framework of the absorption model, that the high-energy experimental data for II³⁹ can be largely reproduced if the OPE inelastic partial-wave cross sections are substantially reduced for classical impact parameters less than about 1 F. This suppression is interpreted as due to unitarity limitations. It seems likely that a corresponding "unitarity suppression" will also effect the OPE exchange amplitude for II and III at intermediate energies where the absorption model is no longer valid.⁴⁰

In the absorption-model treatment of reaction II,³⁹ inelastic partial-wave amplitudes are multiplied by a factor

$$[(1-e^{-\nu b^2})(1-e^{-\nu' b^2})]^{1/2}, \quad (3.1)$$

where b is the classical impact parameter. The parameters ν and ν' are associated with the widths of the elastic-scattering diffraction peaks in the initial and final channels, and the Gaussian form of the "cutoffs" comes from the fact that the diffraction peaks have a characteristic Gaussian dependence upon momentum transfer.

This parametrization of the absorption model suggested to us that we might be able to represent the unitarity-suppression effects on the OPE amplitude at intermediate energies by a cutoff factor

$$1-e^{-Ar^2} \quad (3.2)$$

with the same dependence upon r as the cutoff factor (3.1) has on b when $\nu=\nu'=A$. Our test of this idea was to compare the Born-approximation production cross sections, obtained from the cutoff OPE transition potential, with the experimental data as parametrized by the Ferrari-Selleri (F-S) model⁵ for reaction II and the Ferrari model (F)⁶ for reaction III. We obtain an excellent fit to the F-S model for reaction II with $A_{\text{II}}=1.5\mu_\pi^2$ and to the F model for reaction III with $A_{\text{III}}=1.1\mu_\pi^2$. The fit is to within a few percent for momentum transfers in the interval in which most of the experimental events fall at intermediate energies, -2 to $-10m_\pi^2$. It is interesting to note that the r dependence of the resulting cutoff factor [Eq. (3.2)]

³⁹ G. Alexander, B. Haber, A. Shapira, and G. Yekutieli, Phys. Rev. 144, 1122 (1966).

⁴⁰ In these energy regions the unmodified OPE Born amplitudes for reaction II by itself exceeds partial-wave unitarity bounds.

for reaction II is almost identical to the b dependence of (3.1) when ν is fixed by p - p scattering and ν' is adjusted to fit absorption-model predictions to experiment at high energies.³⁹

We have not made any estimates of the transition potential coupling the N - $\Delta(1236)$ to the $\Delta(1236)$ - $\Delta(1236)$ channel or the diagonal potentials in the N - $\Delta(1236)$ or $\Delta(1236)$ - $\Delta(1236)$ channels. We will ultimately neglect these potentials and will judge the validity of this approximation on the basis of the assumption that the neglected potentials are approximately of the same magnitude as those which have been estimated.

Our diagonal potentials in the N - N channel will be taken to be the sum of the OPEP and the vector-meson-exchange potential which we have calculated in Sec. 2.

Coupled-Channel Calculation

Our wave function describing the N - N scattering state must include components to describe the coupled amplitudes of all the virtual N - $\Delta(1236)$ and $\Delta(1236)$ - $\Delta(1236)$ states with the quantum numbers I , J , and P . We will adopt the following notation to distinguish the various amplitudes:

A component of the state wave function ψ will be labeled $\psi_{(N,L,S)}^{(I,J,P,M)}(r)$. The subscript N indicates the channel number; N - N , N - $\Delta(1236)$, $\Delta(1236)$ - $\Delta(1236)$ correspond to 1, 2, 3, respectively. The superscript I indicates the isospin, P the parity, and the four indices J , M , L , and S indicate the total angular momentum, its z component, the orbital angular momentum, and the spin angular momentum, respectively.⁴¹ The final dependence of ψ is on the magnitude of the particle separation r in the channel.⁴² In what follows we will not write down the superscripts I , P , J , and M explicitly since they will be unaffected by the discussion.

The Schrödinger equation for ψ is

$$(H_0 - E)\psi = -V\psi, \quad (3.3a)$$

where

$$H_0 = \sum_{N=1,3} (T_N + M_N - 2M) \quad (3.3b)$$

is the free Hamiltonian which depends only upon the channel number N , and is independent of the indices I , J , M , L , and S . It contains a kinetic-energy term plus a mass term.⁴³ We have chosen the zero of energy

⁴¹ For example, when $J=L$, $P=+$, $I=0$, $M=1, 0$, or -1 , the subvector ψ with $N=1$ has two components associated with the 3S_1 and 3D_1 N - N states, respectively; the subvector of ψ with $N=3$ has components associated with the $\Delta(1236)$ - $\Delta(1236)$ 3S_1 , 3D_1 , 1D_1 , and 1G_1 states, respectively, and the subvector of ψ with $N=2$ has no components.

⁴² The dependence of ψ on the orientation of this separation can be reconstructed from the indices J , M , L , and S .

⁴³ We do not have to write down the explicit derivative form of the kinetic-energy operator at this stage. Ultimately, we will operate with T_2 and T_3 on a complete set of free states in channels

to be at the N - N threshold. The mass terms in the channels 2 and 3, therefore, represent the distance of these thresholds above the N - N threshold,

$$\begin{aligned} M_2 - 2M &= M^* - M \approx 300 \text{ MeV}, \\ M_3 - 2M &= 2(M^* - M) \approx 600 \text{ MeV}, \end{aligned} \quad (3.3c)$$

and set the scale which will be used in our discussion of the relative importance of the various terms in V .

Writing out Eq. (3.3a) explicitly in terms of (N, L, S) indices and r dependence, we have

$$\begin{aligned} [H_0 - E]_{NLS, N'L'S'} \psi_{(N'L'S')}(r) \\ = -[V(r)]_{NLS, N'L'S'} \psi_{(N'L'S')}(r). \end{aligned} \quad (3.4)$$

The matrix elements of these potentials within a particular (N, N') submatrix are calculated as follows:

$$\begin{aligned} [V(r)]_{NLS, N'L'S'} \\ = \sum_{MLMS_1 S_2 S_3 S_4} \langle JM | LM_L SM_S \rangle^* \langle JM | L'M_L' S'M_S' \rangle \\ \times \int d \cos \theta d \phi [Y_L^{ML}(\theta, \phi)]^* [\chi_{S'}]_{S_3 S_4} \\ \times [V(r, \theta, \phi)]_{S_3 S_4, S_1 S_2} [\chi_S]_{S_1 S_2} Y_L^{M'L'}(\theta, \phi), \end{aligned} \quad (3.5)$$

where $\chi_S, \chi_{S'}$ are initial and final spin wave functions whose spin indices are contracted with the spin indices of V .

We turn now to the primary concern of this section, which is to describe the approximations by which we derive an effective potential in the N - N channel representing the effect of the coupling to the closed higher channels.⁴⁴

Equation (3.4) gives

$$\begin{aligned} \psi_2 &= -[(H_0 - E)_{22} + V_{22}]^{-1} [V_{21}\psi_1 + V_{23}\psi_3], \\ \psi_3 &= -[(H_0 - E)_{33} + V_{33}]^{-1} [V_{31}\psi_1 + V_{32}\psi_2], \end{aligned} \quad (3.6)$$

where only the indices (N, N') are shown.⁴⁵ One may solve Eq. (3.6) for ψ_2 in terms of ψ_1 by the formal

II and III and will assume that they give the relativistic kinetic energies in these channels. Since the purpose of this discussion is to reduce the coupled-channel Schrödinger equation to an equivalent Schrödinger equation in the N - N channel, we will not use an explicit T_1 . However, we compare our resulting effective potentials to the phenomenological potentials of Reid, who used the usual nonrelativistic form for T_1 .

⁴⁴ Our approximation will be virtually identical to that used successfully by T. T. S. Kuo and G. E. Brown, Phys. Letters 18, 54 (1965) in deriving an effective attraction in the 3S_1 state due to coupling to the 3D_1 state. The role of the N - $\Delta(1236)$ mass splitting, which makes our effective N - N interaction attractive (coupling to a higher channel), is played in Kuo and Brown's application by the centrifugal barrier in the 3D_1 state which results in the 3D_1 states which contribute most strongly to the low-energy 3S_1 attraction being about 200 MeV above N - N threshold.

⁴⁵ Therefore, each element $(H_0 - E)_{N'N}$ and $V_{N'N}$ should be understood to be a matrix function of r and its derivatives with indices LS and $L'S'$. Similarly, each wave-function element ψ_N should be understood to be a subvector with indices LS .

expansion

$$\begin{aligned} \psi_2 = & -\{[(H_0-E)_{22}]^{-1}V_{21} \\ & -[(H_0-E)_{22}]^{-1}V_{22}[(H_0-E)_{22}]^{-1}V_{21} \\ & -[(H_0-E)_{22}]^{-1}V_{23}[(H_0-E)_{33}]^{-1}V_{31} + \dots\}\psi_1, \end{aligned} \quad (3.7)$$

where the expansion is seen to be in powers of

$$[(H_0-E)_{NN}]^{-1}V_{NN'}.$$

To estimate how fast this expansion converges, we note that the lowest eigenvalues of $(H_0-E)_{22}$ are of the order of M^*-M . Similarly, the lowest eigenvalues of $(H_0-E)_{33}$ are not much less than $2(M^*-M)$. This is because E is less than m_π for the elastic N - N scattering states of interest to us here. We will assume that the values of $V_{NN'}$ are much smaller than these values of $(H_0-E)_{NN}$. Judging from the magnitudes of the phenomenological N - N potentials found by Reid, this is almost certainly true outside some small radius of the order of 0.3 - $0.4(m_\pi)^{-1}$. Inside this radius the higher channels should be effectively decoupled from the N - N channel by either the large repulsive vector-meson potential which we find contributing to V_1 , for the s states, or by the centrifugal barrier in the higher- L N - N states.⁴⁶

Neglecting the higher-order terms in the expansion (3.7) for ψ_2 and in the corresponding expansion for ψ_3 , we have

$$\begin{aligned} \psi_2 = & -[(H_0-E)_{22}]^{-1}V_{21}\psi_1, \\ \psi_3 = & -[(H_0-E)_{33}]^{-1}V_{31}\psi_1. \end{aligned} \quad (3.8)$$

Substituting in the expression obtained from Eq. (3.4),

$$(H_0-E)_{11}\psi_1 = -V_{11}\psi_1 - V_{21}\psi_2 - V_{31}\psi_3, \quad (3.9)$$

we find

$$\begin{aligned} (H_0-E)_{11}\psi_1 = & -\{V_{11} - V_{12}[(H_0-E)_{22}]^{-1}V_{21} \\ & - V_{13}[(H_0-E)_{33}]^{-1}V_{31}\}\psi_1. \end{aligned} \quad (3.10)$$

This gives us an expression in which the amplitudes of the virtual states no longer appear explicitly. The contributions of the coupled channels are not yet in the form of effective potentials depending on r , however, since H_0 contains derivatives and $[(H_0-E)_{NN}]^{-1}$ is, consequently, not a useful operator.

Inserting a complete set of eigenfunctions of (H_0-E) in the coupled-channel terms in Eq. (3.10), we may

⁴⁶ These are plausibility arguments to justify our neglect of all but the first term in the expression (3.7) for ψ_2 and in the corresponding expression for ψ_3 . We would be the first to agree, however, that a consideration of the higher terms (which would necessitate a calculation of V_2^2 , V_3^2 , V_3^3 , and V_2^3) might be a logical next step in the development of calculations of the N - N potential. Whether the Schrödinger framework is the most suitable one within which to pursue this next step is another question. We believe that higher-order calculations may be more sensitive to the inadequacy of the Schrödinger equation as a dynamical formalism than the lowest-order calculation considered here.

rewrite

$$\begin{aligned} V_{1N}[(H_0-E)_{NN}]^{-1}V_{N1} \\ = \int dn V_{1N}|n\rangle \frac{1}{E_N(n)-E} \langle n|V_{N1}, \end{aligned} \quad (3.11)$$

where N equals 2 or 3. We take the complete set $\{|n\rangle\}$ to be

$$\{|n\rangle\} = \{ \langle JM | LM_L SM_s \rangle Y_L^{ML}(\theta, \phi) j_L(kr) \}. \quad (3.12)$$

The energies are then functions of k , e.g., $E_2(n) = E_2(k)$. Making these substitutions in Eq. (3.10), we obtain

$$\begin{aligned} V_{1N}[(H_0-E)_{NN}]^{-1}V_{N1}\psi_1 \\ = \sum_{L'S'} \int \frac{k^2 dk}{E_N(k)-E} [V(r)]_{ILS, NL'S'} j_{L'}(kr) \\ \times \int (r')^2 dr' j_{L'}(kr') \\ \times [V(r')]_{NL'S', 1L'S'} \psi_{1L'S'}(r'), \end{aligned} \quad (3.13)$$

which, substituted in Eq. (3.9), gives an integro-differential matrix equation for ψ_1 .

Completeness Approximation

We come finally to the completeness approximation argument by which it is possible to turn the integral expressions (3.13) into the form of an effective potential times ψ_1 . The completeness approximation is appropriate because we will find that the integrands in the k integrals in Eq. (3.13) are peaked about definite values of k . This peaking makes it a reasonable approximation to take the energy denominators out from inside the k integrals,

$$E_N(k)-E \rightarrow E_{N,LS,L'S',L''S''}-E,$$

where $E_{N,LS,L'S',L''S''}$ are the values of $E_2(k)$, $E_3(k)$ at the peaks of the various k integrands in Eq. (3.13). The k integrations become trivial,

$$\int k^2 dk j_{L'}(kr) j_{L'}(kr') = \delta(r-r') r^{-2},$$

giving a result which makes the r' integrations trivial in turn. Thus, as a result of the completeness approximation, we have

$$\begin{aligned} V_{1N}[(H_0-E)_{22}]^{-1}V_{N1}\psi_1 \\ = \sum_{NL'S'} -[V(r)]_{ILS, NL'S'} \frac{1}{E_{N,LS,L'S',L''S''}-E} \\ \times [V(r)]_{NL'S', 1L'S'} \psi_{1L'S'}(r). \end{aligned} \quad (3.14)$$

When these expressions are substituted in Eq. (3.9),

they give us

$$\begin{aligned}
(H_0 - E)\psi_{1LS}(r) = & - \sum_{L',S'} \left\{ [V(R)]_{1LS,1L'S''} \right. \\
& - [V(r)]_{1LS,2L'S'} \frac{1}{E_{2,LS,L'S',L''S''} - E} [V(r)]_{2L'S',1L''S''} \\
& - [V(r)]_{1LS,3L'S'} \frac{1}{E_{3,LS,L'S',L''S''} - E} \\
& \left. \times [V(r)]_{3L'S',1L''S''} \right\} \psi_{1L''S''}(r). \quad (3.15)
\end{aligned}$$

It only remains to demonstrate the validity of the completeness approximation and to determine the values of $E_{N,LS,L'S',L''S''}$. The second Born-approximation contribution of the states $|NL'S'\rangle$ to the scattering between interacting N - N states is just proportional to the integral over E_N of

$$\begin{aligned}
& k^2 \frac{dk}{dE_N} \frac{1}{E_N - E} \int d^3r \psi_{1LS}^\dagger(r) V_{1LS,NL'S'} j_{L'}(kr) \\
& \times \int d^3r' j_{L'}(kr') V_{NL'S',1L''S''} \psi_{1L''S''}(r'). \quad (3.16)
\end{aligned}$$

The reader will recognize this amplitude as the right-hand side of Eq. (3.13) multiplied by $\psi_{1LS}^\dagger(r)$ and integrated over r . We will show that the completeness approximation is valid for this amplitude.

With the exception of the s -wave phase shifts, all the partial-wave phase shifts for N - N scattering in the elastic region are relatively small relative to 90° . It was thought reasonable for our purposes, therefore, to approximate

$$\begin{aligned}
\psi_{1LS}(r) &= j_L(pr), \quad L \neq 0, \\
\psi_{1L''S''}(r') &= j_{L''}(pr'), \quad L'' \neq 0,
\end{aligned}$$

where p is the momentum in the N - N channel associated with the energy E . For the cases L or $L''=0$, where the phase shifts are large at low energies, the approximation

$$\psi_{10S}(r) = \left\{ \sin[\delta_S(p)] - e^{-\alpha_S(r-r_0)} \sin[\delta_S(p)] \right\} \theta(r-r_0)/pr$$

was used. Here $\delta_S(p)$ was evaluated in the effective range approximation

$$\cot \delta_S(p) = -1/a_S p + \frac{1}{2} r_S p,$$

which holds in the energy interval where both the experimental and the effective range approximation phase shifts are large. The parameter r_0 represents an effective hard-core radius chosen at $r_0 = 0.35 m_\pi^{-1}$ and α_S is fixed at

$$\alpha_0 = 2.02 \text{ F}^{-1}, \quad \alpha_1 = 2.96 \text{ F}^{-1},$$

by the requirement that $\psi_{10S}(r)$ be consistent with the experimental effective range.

The integrals (3.16) were found to be sharply peaked as a function of $E(k)$ with a small half-width of the order of 50–100 MeV compared to a peak position of the order 450 MeV for $N=2$ and 700 MeV for $N=3$. For $(L'',S'')=(L,S)$, it was found that the values of the energy denominators $E_{N,LS,L'S',LS}-E$ could be well represented to within 10 or 20 MeV by the phenomenological forms

$$\begin{aligned}
& E_{N,LS,L'S',LS}-E \\
& = \bar{E}_N + (m_\pi)^2 [L'(L'+1) - L(L+1)]/M (b_N)^2
\end{aligned}$$

for $L' \geq L$ and

$$E_{N,LS,L'S',LS}-E = (\Delta M)_N + 25 - T$$

for $L' < L$, where

$$\bar{E}_2 = 335 \text{ MeV}, \quad \bar{E}_3 = 610 \text{ MeV},$$

and the parameter b_N is a phenomenological impact parameter given, in units of $(m_\pi)^{-1}$, by

$$\begin{aligned}
(b_2)^2 &= \frac{1.2 m_\pi}{M} \frac{[2 + (L+1)(L'+1)]}{1.16 + T/m_\pi}, \\
(b_3)^2 &= \frac{2.32 m_\pi}{M} \frac{[0.7 + (L+1)(L'+1)]}{1.746 + T/m_\pi}.
\end{aligned}$$

The symbol T denotes the kinetic energy in MeV in the N - N channel and $(\Delta M)_N$ is the energy difference in MeV between the N - N threshold and the thresholds of channels II and III. When $L'' \neq L$, it was found that $E_{N,LS,L'S',L''S''}$ was given adequately by the approximation

$$E_{N,LS,L'S',L''S''} = \frac{1}{2} [E_{N,LS,L'S',LS} + E_{N,L''S'',L'S',L''S''}].$$

ACKNOWLEDGMENTS

Much of this work was done while the authors were at the Newman Laboratory for Nuclear Studies, Cornell University. We would like to thank our friends there for many stimulating conversations. We especially thank H. A. Bethe for his constant encouragement and R. Reid for his permission to reproduce his phenomenological potentials before their publication.

APPENDIX A: VECTOR-MESON-EXCHANGE BORN AMPLITUDE AND POTENTIAL

Born Amplitudes

The invariant Born amplitude for the vector-meson-exchange diagram shown in Fig. 6 may be written

$$\begin{aligned}
& \mathfrak{M}(p_3 S_3, p_4 S_4; p_1 S_1, p_2 S_2) \\
& = -i \Gamma^\mu(p_3 S_3, p_1 S_1) \frac{-g_{\mu\nu} + q_\mu q_\nu}{q^2 - m^2 + i\epsilon} \Gamma^\nu(p_4 S_4, p_2 S_2), \quad (A1)
\end{aligned}$$

where

$$q_\mu = (p_3 - p_1)_\mu$$

and m is the mass of the meson. The vertex factors Γ^μ in this expression may be written in terms of the sum of electric and Dirac matrix elements

$$\Gamma^\mu(p'S', pS) = A_E \bar{U}(p'S') (P^\mu/2M) U(pS) + A_D \bar{U}(p'S') \gamma^\mu U(pS), \quad (\text{A2})$$

where

$$P^\mu = (p' + p)^\mu$$

and M is the mass of the baryon. (We neglect vector-meson and baryon mass splittings.) The coefficients A_E and A_D are related to the electric and magnetic and $SU(3)$ structure constants defined in Sec. 3:

$$\begin{aligned} A_E &= G_E g^{abc}(f_E, d_E) - G_M g^{abc}(f_M, d_M), \\ A_D &= (1 - q^2/4M^2) G_M g^{abc}(f_M, d_M). \end{aligned} \quad (\text{A3})$$

Using $q_\mu \Gamma^\mu(p'S', pS) = 0$, the matrix element may be rewritten

$$\mathfrak{N} = i(q^2 - m^2 + i\epsilon)^{-1} j^\mu(p_3 S_3, p_1 S_1) j_\mu(p_4 S_4, p_2 S_2). \quad (\text{A4})$$

When \mathfrak{N} is evaluated in the c.m. frame, where

$$\begin{aligned} p_1 &= (\mathbf{p}, E), & p_2 &= (-\mathbf{p}, E), \\ p_3 &= (\mathbf{p}', E), & p_4 &= (-\mathbf{p}', E), \end{aligned}$$

we obtain

$$\begin{aligned} & j^\mu(p_3 S_3, p_1 S_1) j_\mu(p_4 S_4, p_2 S_2) \\ &= [A_E^2 (2E^2/M^2 - 1 + q^2/4M^2) - 2A_E A_D] D_1 \\ & \quad + (2E/M) A_E A_D D_3 + A_D^2 (D_2 + D_4). \end{aligned} \quad (\text{A5})$$

The D_i are the products of Dirac matrix elements

$$\begin{aligned} D_1 &= [\bar{U}(\mathbf{p}'S_3) U(\mathbf{p}S_1)] [\bar{U}(-\mathbf{p}'S_4) U(-\mathbf{p}S_2)], \\ D_2 &= [\bar{U}(\mathbf{p}'S_3) \gamma_0 U(\mathbf{p}S_1)] [\bar{U}(-\mathbf{p}'S_4) \gamma_0 U(-\mathbf{p}S_2)], \\ D_3 &= [\bar{U}(\mathbf{p}'S_3) U(\mathbf{p}S_1)] [\bar{U}(-\mathbf{p}'S_4) \gamma_0 U(-\mathbf{p}S_2)] \\ & \quad + [\bar{U}(\mathbf{p}'S_3) \gamma_0 U(\mathbf{p}S_1)] [\bar{U}(-\mathbf{p}'S_4) U(-\mathbf{p}S_2)], \\ D_4 &= \sum_{i=1,3} -[\bar{U}(\mathbf{p}'S_3) \gamma_i U(\mathbf{p}S_1)] \\ & \quad \times [\bar{U}(-\mathbf{p}'S_4) \gamma_i U(-\mathbf{p}S_2)]. \end{aligned} \quad (\text{A6})$$

These matrix elements may be further expanded by expressing the Dirac spinors in terms of two-component

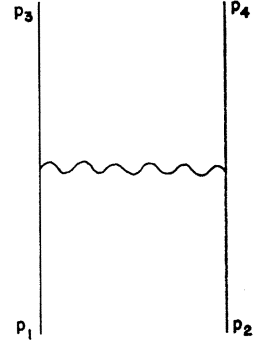


FIG. 6. Labeling of particle lines in vector-meson-exchange diagram.

Pauli spinors χ_a as

$$U(\mathbf{p}S_a) = [2M(E+M)]^{-1/2} [(E+M)\chi_a, \boldsymbol{\sigma} \cdot \mathbf{p}\chi_a], \quad (\text{A7})$$

where the Pauli spinors are normalized to unity. This expansion gives the D_i in terms of the products of Pauli matrices

$$\begin{aligned} S_c &= (\chi_{s_3}^\dagger \chi_{s_1}) \cdot (\chi_{s_4}^\dagger \chi_{s_2}), \\ S_{\sigma\sigma} &= (\chi_{s_3}^\dagger \boldsymbol{\sigma} \chi_{s_1}) \cdot (\chi_{s_4}^\dagger \boldsymbol{\sigma} \chi_{s_2}), \\ S_T &= 3[(\chi_{s_3}^\dagger \boldsymbol{\sigma} \chi_{s_1}) \cdot \mathbf{q}] [(\chi_{s_4}^\dagger \boldsymbol{\sigma} \chi_{s_2}) \cdot \mathbf{q}] - |\mathbf{q}|^2 S_{\sigma\sigma}, \\ S_{LS} &= i(\mathbf{p}' \times \mathbf{p}) \cdot [\frac{1}{2}(\chi_{s_3}^\dagger \boldsymbol{\sigma} \chi_{s_1}) + \frac{1}{2}(\chi_{s_4}^\dagger \boldsymbol{\sigma} \chi_{s_2})], \\ S_{LS2} &= [(\chi_{s_3}^\dagger \boldsymbol{\sigma} \chi_{s_1}) \cdot (\mathbf{P} \times \mathbf{q})] [(\chi_{s_4}^\dagger \boldsymbol{\sigma} \chi_{s_2}) \cdot (\mathbf{P} \times \mathbf{q})]. \end{aligned} \quad (\text{A8})$$

The matrix relating the D_i to the S 's is given in Table I.

Potentials

The nonrelativistic potential corresponding to the invariant amplitude is conveniently defined as

$$V(\mathbf{r}) = \frac{i}{(2\pi)^3} \int \mathfrak{N}(\mathbf{q}, E, S_1, S_2, S_3, S_4) e^{i\mathbf{q} \cdot \mathbf{r}} d\mathbf{q}. \quad (\text{A9})$$

We will express this potential in terms of the conventional decomposition

$$V(\mathbf{r}, E) = V_c(S, E) \mathbf{1}_1 \mathbf{1}_2 + V_{\sigma\sigma}(\mathbf{r}, E) \boldsymbol{\sigma}_1 \boldsymbol{\sigma}_2 + V_T(\mathbf{r}, E) S_{12} + V_{LS}(\mathbf{r}, E) \mathbf{L} \cdot \mathbf{S} + V_Q(\mathbf{r}, E) Q_{12}, \quad (\text{A10})$$

where

$$\begin{aligned} S_{12} &= 3(\boldsymbol{\sigma}_1 \cdot \hat{r})(\boldsymbol{\sigma}_2 \cdot \hat{r}) - \boldsymbol{\sigma}_1 \cdot \boldsymbol{\sigma}_2, \\ \mathbf{S} &= \frac{1}{2}[\boldsymbol{\sigma}_1 \mathbf{1}_2 + \mathbf{1}_1 \boldsymbol{\sigma}_2], \\ Q_{12} &= \frac{1}{2}[(\mathbf{L} \cdot \boldsymbol{\sigma}_1)(\mathbf{L} \cdot \boldsymbol{\sigma}_2) + (\mathbf{L} \cdot \boldsymbol{\sigma}_2)(\mathbf{L} \cdot \boldsymbol{\sigma}_1)], \end{aligned}$$

TABLE I. Matrix relating Dirac matrix elements to Pauli matrix elements.^a

Pauli	S_c	$S_{\sigma\sigma}$	S_T	S_{LS}	S_{LS2}
Dirac					
D_1	$[2M(E+M) - \frac{1}{2}q^2]^2$	0	0	$-4M(E+M) - \frac{1}{2}q^2$	-1
D_2	$[2E(E+M) + \frac{1}{2}q^2]^2$	0	0	$4E(E+M) + \frac{1}{2}q^2$	-1
D_3	$[2E(E+M) + \frac{1}{2}q^2][2E(E+M) - \frac{1}{2}q^2]$	0	0	$2[-q^2 + 2(M-E)^2]$	+2
D_4	$(E+M)^2(4E^2 - 4M^2 + q^2)$	$-\frac{2}{3}(E+M)^2$	$\frac{1}{3}(E+M)^2$	$4(E+M)^2$	0

^a An over-all normalization factor of $[2M(E+M)]^{-2}$ has been factored out.

and we have used the notation $(\mathbf{I}_1, \boldsymbol{\sigma}_1)$, $(\mathbf{I}_2, \boldsymbol{\sigma}_2)$ for the 2×2 unit and Pauli spin matrices relating the possible spin states of the particle pairs (1,3) and (2,4), respectively. The coefficients $V(r, E)$ are scalar functions of r and E and contain implicitly the coupling constants and $SU(3)$ structure factors.

The evaluation of the Fourier transform is mostly conventional and straightforward. We summarize the results here in terms of the correspondence between the various factors in \mathfrak{M} and V : (a)

$$q^2 \rightarrow m^2$$

except, of course, in the denominators; (b) the factors of 2π and 4π give the net result

$$G_E \rightarrow G_E/\sqrt{(4\pi)}, \quad G_M \rightarrow G_M/\sqrt{(4\pi)};$$

and (c) the denominators and S 's are transformed according to

$$(q^2 - m^2)^{-1} S_c \rightarrow -m Y_0(x) \mathbf{I}_1 \mathbf{I}_2, \quad (\text{A11a})$$

$$(q^2 - m^2)^{-1} S_{\sigma\sigma} \rightarrow -m Y_0(x) \boldsymbol{\sigma}_1 \cdot \boldsymbol{\sigma}_2, \quad (\text{A11b})$$

$$(q^2 - m^2)^{-1} S_T \rightarrow m^3 x^2 Y_2(x) S_{12}, \quad (\text{A11c})$$

$$(q^2 - m^2)^{-1} S_{LS} \rightarrow -m^3 Y_1(x) \mathbf{L} \cdot \mathbf{S}, \quad (\text{A11d})$$

$$(q^2 - m^2)^{-1} S_{LS2} \rightarrow m^5 Y_2(x) Q_{12}$$

$$\begin{aligned} & -\frac{1}{3} m^3 \left\{ \left[|\mathbf{p}|^2 - (m^2/16x^2) [L'(L'+1) \right. \right. \\ & \left. \left. - L(L+1)]^2 + \frac{1}{2} m^2 \right\} Y_1(x) - \frac{5}{2} m^2 Y_2(x) \right. \\ & \left. + m^2/4x^2 [L'(L'+1) - L(L+1)] (L-L') \right. \\ & \left. \times \left[1 + \frac{2|\mathbf{p}|^2}{m^2} \frac{x^2}{(2L+3)(2L'+3)} \right] Y_1(x) \right\} S_{12} \\ & + \frac{1}{3} m^3 \left[(-2|\mathbf{p}|^2 - m^2) Y_1(x) \right. \\ & \left. + 2m^2 Y_2(x) \right] \boldsymbol{\sigma}_1 \cdot \boldsymbol{\sigma}_2, \quad (\text{A11e}) \end{aligned}$$

where

$$x = mr,$$

$$Y_0(x) = e^{-x}/x,$$

$$Y_1(x) = -\frac{1}{x} \frac{d}{dx} Y_0(x) = -\left(\frac{1}{x^2} + \frac{1}{x} \right) Y_0(x),$$

$$Y_2(x) = \left(\frac{1}{x} \frac{d}{dx} \right)^2 Y_0(x) = \left(\frac{3}{x^4} + \frac{3}{x^3} + \frac{1}{x^2} \right) Y_0(x),$$

and L' and L are, respectively, the final and initial orbital angular momenta. The terms in (A11e) correspond to the last two terms of (2.8). In Sec. 2 we have discussed the difficulty of replacing these (previously neglected) terms by potentials not containing derivative terms. This difficulty is apparent in the complexity

of the right-hand side of (A11e). It may be seen that the terms on the right-hand side of (A11e) have a very singular r dependence. Consequently, these terms are important at small r even though their coefficients are smaller by a factor $(m/2M)^4 \approx 0.02$ than the coefficients of the leading terms in the potential. In particular, they account for the N - N repulsive cores in the s waves, where the leading terms cancel (see Sec. 2).

It must be obvious to the reader that a considerable amount of manipulation went into obtaining the Fourier transform of S_{LS2} . The purpose was to obtain an operator free of momentum-dependent terms such as $(\boldsymbol{\sigma}_1 \times \mathbf{P}) \cdot (\boldsymbol{\sigma}_2 \times \mathbf{P})$. Such momentum-dependent terms have been transformed into L, L' , and energy-dependent terms. (We refer to the $|\mathbf{p}|^2$ as energy-dependent terms since we will use the substitution

$$|\mathbf{p}|^2 = E^2 - M^2,$$

rather than

$$|\mathbf{p}|^2 = -\nabla^2,$$

in evaluating the potentials. That this corresponds to a choice of off-mass-shell behavior, which is arbitrary without a more complete theory, has been commented upon in Sec. 3.) We reproduce here our derivation of the Fourier transform of $(m^2 - q^2)^{-1} S_{LS2}$.

The first step is straightforward:

$$\begin{aligned} & \frac{1}{4} \int \frac{\boldsymbol{\sigma}_1 \cdot (\mathbf{P} \times \mathbf{q}) \boldsymbol{\sigma}_2 \cdot (\mathbf{P} \times \mathbf{q})}{|\mathbf{q}|^2 + m^2} e^{i\mathbf{q} \cdot \mathbf{r}} d\mathbf{q} \\ & = -(\boldsymbol{\sigma}_1 \times \mathbf{P}) \cdot (\boldsymbol{\sigma}_2 \times \mathbf{P}) \frac{1}{4} m^2 Y_1(x) \\ & \quad - [\boldsymbol{\sigma}_1 \cdot (\mathbf{r} \times \mathbf{P})][\boldsymbol{\sigma}_2 \cdot (\mathbf{r} \times \mathbf{P})] m^5 Y_2(x). \quad (\text{A12}) \end{aligned}$$

We wish now to replace \mathbf{P} by derivatives. Since $\mathbf{P} = \mathbf{p}' + \mathbf{p}$, it can be replaced by the sum of two gradients operating upon the final and initial wave functions. In this way, we have, after integration by parts,

$$\begin{aligned} \mathbf{P}_i \mathbf{P}_j (Y_1(x)/m^2) & = -\{ \nabla_i, \{ \nabla_j, (Y_1(x)/m^2) \} \} \\ & = \delta_{ij} Y_2(x) + \hat{r}_i \hat{r}_j x^2 Y_3(x) \\ & \quad - 2\{ \nabla_i \nabla_j, (Y_1(x)/m^2) \}, \quad (\text{A13a}) \end{aligned}$$

where

$$x^2 Y_3(x) \equiv x dY_2(x)/dx = -5Y_2(x) + Y_1(x). \quad (\text{A13b})$$

The curly brackets stand for anticommutators and the gradients are understood to operate on the Yukawa function and the initial wave function. Using Eqs. (A13), we may express the first term in our Fourier transform as

$$\begin{aligned} & -\frac{1}{4} (\boldsymbol{\sigma}_1 \times \mathbf{P}) (\boldsymbol{\sigma}_2 \times \mathbf{P}) m^2 Y_1(x) \\ & = \frac{1}{4} m^4 \{ [- (5/3) Y_2(x) + \frac{1}{3} Y_1(x)] S_{12} \\ & \quad + [\frac{4}{3} Y_2(x) - (p^2/m^2) Y_1(x) - \frac{2}{3} Y_1(x)] \boldsymbol{\sigma}_1 \cdot \boldsymbol{\sigma}_2 \\ & \quad + \frac{1}{2} m^2 \{ (\boldsymbol{\sigma}_1 \cdot \nabla) (\boldsymbol{\sigma}_2 \cdot \nabla), Y_1(x) \} \}. \quad (\text{A14}) \end{aligned}$$

It is still necessary to reduce the term proportional to

$$\{(\boldsymbol{\sigma}_1 \cdot \nabla)(\boldsymbol{\sigma}_2 \cdot \nabla), Y_1(x)\}$$

in this expression. We go about this reduction by making the substitutions

$$(\boldsymbol{\sigma}_1 \cdot \nabla)(\boldsymbol{\sigma}_2 \cdot \nabla) = \frac{1}{8}[\nabla^2, [\nabla^2, (\boldsymbol{\sigma}_1 \cdot \mathbf{r})(\boldsymbol{\sigma}_2 \cdot \mathbf{r})]], \quad (\text{A15})$$

$$\nabla^2 = r^{-1} d^2 r / dr^2 - L^2 / r^2 \equiv \Delta_r - L^2 / r^2. \quad (\text{A16})$$

Using the decomposition of the Laplacian (A16) and integrating by parts, we reduce this expression to

$$\begin{aligned} \{(\boldsymbol{\sigma}_1 \cdot \nabla)(\boldsymbol{\sigma}_2 \cdot \nabla), Y_1(x)\} &= (1/24)[L^2, [L^2, S_{12} Y_1(x)]] \\ &- |\mathbf{p}|^2 (\frac{1}{3} S_{12} + \boldsymbol{\sigma}_1 \cdot \boldsymbol{\sigma}_2) Y_1(x) \\ &- \left[L^2, \left(Y_1(x) \frac{1}{r} \frac{\partial}{\partial r} - \frac{\partial}{\partial r} \frac{1}{r} Y_1(x) \right) (\frac{1}{3} S_{12} + \boldsymbol{\sigma}_1 \cdot \boldsymbol{\sigma}_2) \right], \end{aligned} \quad (\text{A17})$$

where the only remaining velocity dependence is in the last term. The arrows above the derivatives in this term indicate whether the derivatives operate in the initial (rightward) or final (leftward) wave functions.

It proved impossible to eliminate these radial derivatives in favor of L or energy-dependent functions. We have therefore approximated their effect by finding a nonderivative operator which gives, to a good approximation, the same Born term. We find, with the substitution

$$\begin{aligned} O &\equiv \frac{\partial}{\partial r} \frac{\partial}{\partial r} \rightarrow O' \\ &= (L-L') \frac{1}{r} \left[1 + \frac{2p^2 r^2}{(2L+3)(2L'+3)} \right], \end{aligned} \quad (\text{A18})$$

that the product

$$j_{L'}(pr) O j_L(pr) \quad (\text{A19})$$

is reproduced to better than 10% out to $N-N$ separations of one-pion Compton wavelength and up to momenta appropriate to the one-pion production threshold. [It is comforting to note that this approximation only affects the 3S_1 - 3D_1 and 3P_2 - 3F_2 transition potentials since the commutator with L^2 gives a factor $L'(L'+1) - L(L+1)$ which is zero for diagonal potentials.]

It remains to discuss the second term in Eq. (A12). By replacing \mathbf{P} by the appropriate anticommutators of gradients we find

$$\begin{aligned} &-[\boldsymbol{\sigma}_1 \cdot (\mathbf{r} \times \mathbf{P})][\boldsymbol{\sigma}_2 \cdot (\mathbf{r} \times \mathbf{P})] Y_2(x) \\ &= \frac{1}{2} \{ \boldsymbol{\sigma}_1 \cdot (\mathbf{r} \times \bar{\nabla}), \{ \boldsymbol{\sigma}_2 \cdot (\mathbf{r} \times \bar{\nabla}), Y_2(x) \} \} \\ &+ \frac{1}{2} \{ \boldsymbol{\sigma}_2 \cdot (\mathbf{r} \times \bar{\nabla}), \{ \boldsymbol{\sigma}_1 \cdot (\mathbf{r} \times \bar{\nabla}), Y_2(x) \} \} \\ &+ \frac{1}{2} (\boldsymbol{\sigma}_1 \times \bar{\nabla}) \cdot (\boldsymbol{\sigma}_2 \times \mathbf{r}) Y_2(x) + \frac{1}{2} (\boldsymbol{\sigma}_1 \times \bar{\nabla})(\boldsymbol{\sigma}_2 \times \mathbf{r}) Y_2(x) \\ &+ \frac{1}{2} Y_2(x) (\boldsymbol{\sigma}_1 \times \mathbf{r}) \cdot (\boldsymbol{\sigma}_2 \times \bar{\nabla}) \\ &+ \frac{1}{2} Y_2(x) (\boldsymbol{\sigma}_2 \times \mathbf{r})(\boldsymbol{\sigma}_1 \times \bar{\nabla}). \end{aligned} \quad (\text{A20})$$

This may be rewritten, using integration by parts, as

$$\begin{aligned} &-[\boldsymbol{\sigma}_1 \cdot (\mathbf{r} \times \mathbf{P})][\boldsymbol{\sigma}_2 \cdot (\mathbf{r} \times \mathbf{P})] Y_2(x) \\ &= -4Q_{12} Y_2(x) - 2\boldsymbol{\sigma}_1 \cdot \boldsymbol{\sigma}_2 Y_2(x) \\ &\quad - \frac{1}{2} (\boldsymbol{\sigma}_2 \times \mathbf{r}) [\boldsymbol{\sigma}_1 \times \bar{\nabla}, Y_2(x)] \\ &\quad - \frac{1}{2} (\boldsymbol{\sigma}_1 \times \mathbf{r}) [(\boldsymbol{\sigma}_2 \times \bar{\nabla}), Y_2(x)]. \end{aligned} \quad (\text{A21})$$

Taking the derivatives and using (A13b), we finally obtain

$$\begin{aligned} &= -4Q_{12} Y_2(x) + [(14/3) Y_2(x) - \frac{4}{3} Y_1(x)] \boldsymbol{\sigma}_1 \cdot \boldsymbol{\sigma}_2 \\ &\quad + [-(5/3) Y_2(x) + \frac{1}{3} Y_1(x)] S_{12}. \end{aligned} \quad (\text{A22})$$

Collecting all the terms we obtain the expression in Eq. (A11).

APPENDIX B: INELASTIC OPE BORN AMPLITUDES, THEIR PHENOMENOLOGICAL CORRECTION, AND THE COUPLED-CHANNEL TRANSITION POTENTIALS

We begin with the spin structure of the $p + \pi^+ \rightarrow \Delta^{++}(1236)$ vertex

$$\frac{f^*}{m_\pi} q_\mu \bar{U}^\mu(p^* s^*) U(p s), \quad (\text{B1})$$

where the Rarita-Schwinger spin wave function for the $\Delta(1236)$ has the form

$$\begin{aligned} [\bar{U}^\mu(p^* s^*)]_i &= [L(p^*)]_\nu^\mu \frac{(P^* \cdot \gamma + M^*)}{[2M^*(E^* + M^*)]^{1/2}} \\ &\quad \times (\frac{3}{2} S^* | 1 r \frac{1}{2} s \rangle (\epsilon_r)^\nu \end{aligned} \quad (\text{B2})$$

and

$$q_\mu = (p^* - p)_\mu.$$

Summation is implied over repeated indices, M^* is the $\Delta(1236)$ mass, and S^* is the z component of its spin in its rest frame before being boosted to the momentum \mathbf{p}^* . The polarization 4-vectors $(\epsilon_r)^\nu$, $r=1, 0, -1$, have only space components in the $\Delta(1236)$ rest frame and are combined by the Clebsch-Gordon coefficient with a two-component Pauli spinor (referred to by the index $s=1, 2$) to give a total spin with $J=\frac{3}{2}$, $J_z=S^*$. We normalize $(\epsilon_r)^\nu$ so that

$$(\epsilon_r)^\nu (\epsilon_{r'})_\nu = -\delta_{rr'}.$$

The "boosting" operator for $(\epsilon_r)^\nu$ is the Lorentz transformation

$$\begin{aligned} [L(\mathbf{p}^*)]_\nu^\mu &= \frac{1}{M^*} \begin{pmatrix} E^* & P_i^* \\ P_j^* & M^* \delta_{ij} + P_i^* P_j^* / (E^* + M^*) \end{pmatrix}, \\ &\quad (i, j=1, 3). \end{aligned} \quad (\text{B3})$$

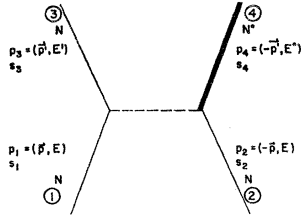


FIG. 7. Labeling of particle lines in $\Delta(1236)$ -production diagram.

The coupling constant f^* can be fixed by setting the first-order expression for the $\Delta(1236)$ decay width

$$\Gamma_{33} = \frac{q^3 (f^*)^2}{24\pi (m_\pi)^2} \frac{[(M^* + M)^2 - (m_\pi)^2]}{(M^*)^2} \quad (\text{B4})$$

equal to the experimental width of 120 MeV. This gives

$$(f^*)^2/4\pi = 0.35.$$

It should be kept in mind, however, that because of the large experimental decay width, the value of f^* determined in this way may not be exactly equal to the effective coupling constant of a real $\Delta(1236)$ going to a real N and a virtual pion. Our qualitative results are not affected by varying $(f^*)^2$ by 20%.

The $p \rightarrow p + \pi^0$ vertex has the spin structure

$$\frac{2fM}{m_\pi} \bar{U}(p', s') \gamma_5 U(p, s),$$

where

$$f^2/4\pi = 0.081.$$

The OPE Born amplitude for reaction II is

$$\mathfrak{M}_{\text{II}} = [iC_{\text{II}}(I) 2f^* f M / (m_\pi)^2] q_\mu [\bar{U}^\mu(p_4 s_4) U(p_2 s_2)] \times [\bar{U}(p_3 s_3) \gamma_5 U(p_1 s_1)] (q^2 - m^2 + i\epsilon)^{-1}. \quad (\text{B5})$$

Here our labeling of 4-momenta (p) and z components of spins (s) follows that in Fig. 7. The factor $C_{\text{II}}(I)$ takes into account the effect of the isospin structure of the vertices which has been ignored thus far,

$$C_{\text{II}}(I) = (8/3)^{1/2}, \quad \text{when } I = 1 \\ = 0, \quad \text{otherwise.}$$

In Eq. (B6) we will reexpress the Dirac spinors for the nucleons in terms of two-component Pauli spinors. We will also reexpress here the Rarita-Schwinger spinor of the $\Delta(1236)$ in terms of a four-component "Pauli spinor" ψ . The four components of this spinor correspond, of course, to the four possible values of S^* in Eq. (B2).

Written in terms of these Pauli spinors, the Born

amplitude becomes, in the c.m. system,

$$\mathfrak{M}_{\text{II}} = iC_{\text{II}}(I) [f^* f / (m_\pi)^2] \{ \chi_3^\dagger [c_1(\boldsymbol{\sigma} \cdot \mathbf{q}) + c_2(\boldsymbol{\sigma} \cdot \mathbf{P})] \chi_1 \} \\ \times \{ \psi_4^\dagger [d_1(\mathbf{S} \cdot \mathbf{q}) + d_2(\mathbf{S} \cdot \mathbf{P}) + id_3(\mathbf{S} \cdot \mathbf{q}) [\boldsymbol{\sigma} \cdot (\mathbf{p}' \times \mathbf{p})] \\ + id_4(\mathbf{S} \cdot \mathbf{P}) [\boldsymbol{\sigma} \cdot (\mathbf{p}' \times \mathbf{p})]] \chi_2 \} (q^2 - m_\pi^2 + i\epsilon)^{-1}. \quad (\text{B6})$$

The labeling of the particle momenta and energies in the c.m. system is indicated in Fig. 7 and

$$\mathbf{P} \equiv (\mathbf{p}' + \mathbf{p}), \quad \mathbf{q} = (\mathbf{p}' - \mathbf{p}).$$

The energy-dependent coefficients c_i and d_i are

$$c_1 = N [\frac{1}{2}(E' + E) + M],$$

$$c_2 = N \frac{1}{2}(E' - E),$$

$$d_1 = \frac{1}{2}(M + M^*)^2 + ME^* + M^*E - \frac{1}{2}q^2,$$

$$d_4 = -\frac{1}{2}[M^{*2} - M^2 + ME^* - ME + \frac{1}{2}q^2] / [M^*(E^* + M^*)],$$

$$d_2 = -\frac{1}{2}d_1 d_4,$$

$$d_3 = -1,$$

and

$$N = [4M^*M(E + M)^2(E + M)(E^* + M^*)]^{-1/2}.$$

We have defined the vector of matrices \mathbf{S} in analogy with the vector of Pauli matrices. In terms of the Clebsch-Gordan coefficients and vectors $\boldsymbol{\epsilon}_m$ introduced in Eq. (B2), \mathbf{S} may be written as

$$(\mathbf{S})_{s^*s} = \sum_m \langle \frac{3}{2} s^* | 1 m \frac{1}{2} s \rangle \boldsymbol{\epsilon}_m.$$

Thus \mathbf{S} has, on the right, a two-component Pauli spinor index and, on the left, a four-component spinor index. The "direction" of \mathbf{S} is associated with the direction of the $\boldsymbol{\epsilon}_m$. There is, of course, an implicit summation over the left-hand index of the σ matrices and the right-hand index of the S matrices in the terms with coefficients d_3 and d_4 in Eq. (B6).

Since this is a qualitative discussion, we have approximated rather freely in obtaining a Schrödinger transition potential from the Born amplitude in Eq. (B6). We have discarded, where great simplifications result, terms of the order of $(M^* - M)/(M^* + M)$ and $p^2/4M^2$. This approximation allows us to discard all but the product proportional to $c_1 d_1$ in the expansion of the right-hand side of Eq. (B6).

In this approximation we have

$$\mathfrak{M}_{\text{II}} = iC_{\text{II}}(I) [f^* f / (m_\pi)^2] G_{\text{II}}(E) [\chi_3^\dagger (\boldsymbol{\sigma} \cdot \mathbf{q}) \chi_1] \\ \times [\psi_4^\dagger (\mathbf{S} \cdot \mathbf{q}) \chi_2] (q^2 - m_\pi^2 + i\epsilon)^{-1}, \quad (\text{B7})$$

where we have defined

$$G_{\text{II}}(E) \equiv c_1 d_1.$$

The OPE Born amplitude for reaction III is, after the same approximations,

$$\mathfrak{N}_{\text{III}} = iC_{\text{III}}(I) [(f^*)^2 / (m_\pi)^2] G_{\text{III}}(E) \times [\psi_3^\dagger(\mathbf{S} \cdot \mathbf{q}) \chi_1] [\psi_4^\dagger(\mathbf{S} \cdot \mathbf{q}) \chi_2], \quad (\text{B8})$$

where

$$G_{\text{III}}(E) = \frac{\{(M^* + M)[E + \frac{1}{2}(M + M^*)]\}^2}{4MM^*(E + M)(E + M^*)}$$

and

$$\begin{aligned} C_{\text{III}}(0) &= \sqrt{2}, \\ C_{\text{III}}(1) &= (10/9)^{1/2}, \\ C_{\text{III}}(I) &= 0 \text{ otherwise.} \end{aligned}$$

Transition Potentials

We calculate transition potentials from the approximate Born amplitudes in Eqs. (B7) and (B8) by the use of Eq. (A9). This gives us

$$V_{\text{II}} = \frac{1}{3} m_\pi \left(\frac{ff^*}{4\pi} \right) C_{\text{II}}(I) G_{\text{II}}(E) \times [S_{12}^{\text{II}} V_2(x_{\text{II}}) - \boldsymbol{\sigma}_1 \cdot \mathbf{S}_2 V_0(x_{\text{II}})],$$

$$V_{\text{III}} = \frac{1}{3} m_\pi \left(\frac{(f^*)^2}{4\pi} \right) C_{\text{III}}(I) G_{\text{III}}(E) \times [S_{12}^{\text{III}} V_2(x_{\text{III}}) - \mathbf{S}_1 \cdot \mathbf{S}_2 V_0(x_{\text{III}})].$$

Here we have written down the potentials in a form so that direct comparison can be made to the elastic OPE exchange amplitude in the N - N channel

$$V_{\text{I}} = \frac{1}{3} m_\pi \left(\frac{f^2}{4\pi} \right) C_{\text{I}}(I) [S_{12}^{\text{I}} V_2(x_{\text{I}}) - \boldsymbol{\sigma}_2 \cdot \boldsymbol{\sigma}_1 V_0(x_{\text{I}})],$$

where

$$C_{\text{I}}(0) = -3, \quad C_{\text{I}}(1) = 1.$$

[For purposes of orientation, the factors $C_{\text{II}}(E)$ and $C_{\text{III}}(E)$ are approximately equal to 1 and vary slowly with E .] The tensor operators are defined by

$$\begin{aligned} S_{12}^{\text{I}} &= 3(\boldsymbol{\sigma}_1 \cdot \hat{r})(\boldsymbol{\sigma}_2 \cdot \hat{r}) - \boldsymbol{\sigma}_1 \cdot \boldsymbol{\sigma}_2, \\ S_{12}^{\text{II}} &= 3(\boldsymbol{\sigma}_1 \cdot \hat{r})(\mathbf{S}_2 \cdot \hat{r}) - \boldsymbol{\sigma}_1 \cdot \mathbf{S}_2, \\ S_{12}^{\text{III}} &= 3(\mathbf{S}_1 \cdot \hat{r})(\mathbf{S}_2 \cdot \hat{r}) - \mathbf{S}_1 \cdot \mathbf{S}_2. \end{aligned}$$

The r -dependent terms in the potentials are defined to have the form

$$V_0(x) \equiv (x^{-1} e^{-x})(x/x_{\text{I}})^2,$$

$$V_2(x) = \left(\frac{3}{x^3} + \frac{3}{x^2} + \frac{1}{x} \right) e^{-x}.$$

The arguments of the potential functions are

$$x_{\text{I}} = x_{\text{III}} = m_\pi r, \quad x_{\text{II}} = m_{\text{II}} r.$$

In reaction II, q^μ has an energy component in the c.m. system,

$$q^0 = E' - E = -(M^{*2} - M^2)/4E.$$

Consequently, the characteristic range parameter m_{II} for V_{II} is not m_π but

$$m_{\text{II}} = [(\Delta E)^2 + (m_\pi)^2]^{1/2}.$$

The matrix elements of S_{12}^{I} and $\boldsymbol{\sigma}_1 \cdot \boldsymbol{\sigma}_2$ between initial and final angular-momentum states are well known. This is not true, however, for the corresponding operators for reactions I and III. It has been necessary for us to reduce these operators to 3- J , 6- J , and 9- J symbols for which tables are available.^{47,48} Our results for the tensor operators are⁴⁹

$$\begin{aligned} \langle JL'S' | S_{12}^{\text{I}} | JLS \rangle &= (-)^{J+S'} [12\sqrt{5}] \\ &\times [(2S+1)(2S'+1)(2L+1)(2L'+1)]^{1/2} \end{aligned}$$

$$\times \begin{pmatrix} L' & L & 2 \\ 0 & 0 & 0 \end{pmatrix} \begin{Bmatrix} 2 & L' & L' \\ J & S & S' \end{Bmatrix} \begin{Bmatrix} \frac{1}{2} & \frac{1}{2} & S \\ \frac{1}{2} & \frac{3}{2} & S' \\ 1 & 1 & 2 \end{Bmatrix},$$

$$\begin{aligned} \langle JL'S' | S_{12}^{\text{III}} | JLS \rangle &= (4\sqrt{30}) [(2S+1)(2S'+1)(2L+1)(2L'+1)]^{1/2} \end{aligned}$$

$$\times \begin{pmatrix} L' & L & 2 \\ 0 & 0 & 0 \end{pmatrix} \begin{Bmatrix} 2 & L' & L' \\ J & S & S' \end{Bmatrix} \begin{Bmatrix} \frac{1}{2} & \frac{1}{2} & S \\ \frac{3}{2} & \frac{3}{2} & S' \\ 1 & 1 & 2 \end{Bmatrix},$$

where the last three factors in each expression are, in

⁴⁷ M. Rotenberg, B. Bivons, N. Metropolis, and J. K. Wooten, Jr., *The 3-J and 6-J Symbols* (Technology Press, Cambridge, Mass., 1957).

⁴⁸ K. Smith and J. W. Stevenson, Argonne National Laboratory Report No. ANL-5776, 1957 (unpublished).

⁴⁹ For those unfamiliar with the uses of these symbols we recommend A. P. Yutsis, I. R. Lennson, and V. V. Vanagas, *Mathematical Apparatus of the Theory of Angular Momentum* (Academy of Science of the Lithuanian S.S.R. Institute of Physics and Mathematics, 1960) (English translation available from Office of Technical Services, U. S. Department of Commerce, Washington 25, D. C., 1962).

order, a 3- J , a 6- J , and a 9- J symbol. We find also that the "spin-spin" operators are proportional to 6- J symbols

$$\langle J'L'S' | \mathbf{S}_1 \cdot \mathbf{S}_2 | JLS \rangle = (-)^{s+1/2} \sqrt{6} \begin{Bmatrix} \frac{3}{2} & \frac{1}{2} & S \\ \frac{1}{2} & \frac{1}{2} & 1 \end{Bmatrix} \delta_{S'S},$$

$$\langle J'L'S' | \mathbf{S}_1 \cdot \mathbf{S}_2 | JLS \rangle = (-)^J \begin{Bmatrix} \frac{1}{2} & \frac{1}{2} & S \\ \frac{3}{2} & \frac{3}{2} & 1 \end{Bmatrix} \delta_{SS'}.$$

In all of these expressions JLS and $J'L'S'$ stand, respectively, for the initial and final state (total, orbital, spin) angular momenta.

Stationary Expectation Values and Slopes of Daughter Regge Trajectories for the Bethe-Salpeter Equation*

RABINDER N. MADAN, RICHARD W. HAYMAKER, AND R. BLANKENBECLER

Department of Physics, University of California, Santa Barbara, California

(Received 25 March 1968)

Variational techniques for the calculation of general expectation values, not just eigenvalues, for the Bethe-Salpeter equation are derived. These formulas are applied to the numerical calculation of Regge trajectories and slopes for a simple potential with spinless particles. The treatment of unequal masses as a perturbation on the equal-mass solutions is also discussed. Particular attention is paid to the problem of crossing trajectories coupled by the perturbation. It is shown that if two unperturbed trajectories cross, then a complex-conjugate pair of trajectories can result in the presence of the perturbation.

I. INTRODUCTION

THE use of the Bethe-Salpeter (BS) equation is a popular theoretical tool to explore the properties of the relativistic scattering amplitude. The properties of Regge trajectories in the case of unequal masses and in the case of nonzero spin and conspiracies have been illuminated by the discussions of the BS equation.¹ Detailed numerical calculations have shown rather spectacular and unexpected behavior of the Regge trajectories in certain cases.² It is useful to have simple perturbation formulas to help in the understanding of such results. To that end, we have formulated variational techniques that work for the calculation of expectation values—not just eigenvalue quantities—for the BS equation. It is important that these techniques be accurate yet analytically as simple as possible.

We start by considering a Rayleigh-Ritz solution of the Bethe-Salpeter equation. Our formulation of stationary expectation values is based on a perturbation treatment of the first-order error in the stationary wave function. This allows one to calculate, for example, trajectory slopes correct to first order in the error of the wave function. It also provides a means of calculating residues to first order. This approach can be applied to the case of particles with spin, and will be in a later paper. These problems can become so complicated that a straightforward numerical approach may

prove to be difficult to understand and to interpret physically.

In Sec. II, the theory of stationary expectation values is presented for the Schrödinger equation and generalized to the Bethe-Salpeter equation in Sec. III. In Sec. IV, we demonstrate the use of the theory in calculating of slopes of daughter Regge trajectories at $s=0$. In Sec. V, a simple numerical example is presented. In Sec. VI, the effect of a mass-difference perturbation on the behavior of equal-mass trajectories is discussed.

II. STATIONARY EXPECTATION VALUES—SCHRÖDINGER THEORY

We address ourselves to the problem of calculating the expectation value of an operator M in a state ψ , $\langle \psi | M | \psi \rangle$, where ψ satisfies the Schrödinger equation $(H-E)\psi=0$. Since the Schrödinger equation cannot generally be solved exactly, we envision obtaining an approximate solution ψ_0 by finding a stationary value of the Rayleigh-Ritz quotient

$$E_0 = \frac{\langle \psi_0 | H | \psi_0 \rangle}{\langle \psi_0 | \psi_0 \rangle}. \quad (2.1)$$

It is well known that the stationary value E_0 differs from the true energy eigenvalue E by terms of second order in $(\psi - \psi_0)$. However, the expectation value of a general operator M ,

$$\langle M \rangle = \frac{\langle \psi_0 | M | \psi_0 \rangle}{\langle \psi_0 | \psi_0 \rangle}, \quad (2.2)$$

* Work supported by the National Science Foundation.

¹ For example, D. Z. Freedman and J. M. Wang, *Phys. Rev.* **153**, 1596 (1967); R. Blankenbecler, R. L. Sugar, and J. D. Sullivan, *ibid.* **172**, 1451 (1968).

² R. E. Cutkosky and B. B. Deo, *Phys. Rev. Letters* **19**, 1256 (1967).